BARD Final Report US-4654-13

Antimicrobial and fouling-resistant membranes for treatment of agricultural and municipal wastewater

Husson, S.M. Clemson University SC
Freger, V. Technion R&D Foundation Ltd.
Herzberg, M. Ben-Gurion University of the Negev

Project award year: 2013
Three year research project

Abstract

This research project introduced a novel membrane coating strategy to combat biofouling, which is a major problem for the membrane-based treatment of agricultural and municipal wastewaters. The novelty of the strategy is that the membrane coatings have the unique ability to switch reversibly between *passive (antifouling)* and *active (antimicrobial)* fouling control mechanisms. This dual-mode approach differs fundamentally from other coating strategies that rely solely on one mode of fouling control.

The research project had two complementary objectives: (1) preparation, characterization, and testing of dual-mode polymer nanolayers on planar surfaces and (2) evaluation of these nanolayers as membrane modifiers. The first objective was designed to provide a fundamental understanding of how polymer nanolayer chemistry and structure affect bacterial deposition and to demonstrate the reversibility of chemical switching. The second objective, which focused on membrane development, characterization, and testing, was designed to demonstrate methods for the production of water treatment membranes that couple passive and active biofouling control mechanisms.

Both objectives were attained through synergistic collaboration among the three research groups. Using planar silicon and glass surfaces, we demonstrated using infrared spectroscopy that this new polymer coating can switch reversibly between the anti-fouling, zwitterion mode and an anti-microbial, quaternary amine mode. We showed that switching could be done more than 50 times without loss of activity and that the kinetics for switching from a low fouling zwitterion surface to an antimicrobial quaternary amine surface is practical for use. While a low pH was required for switching in the original polymer, we illustrated that by slightly altering the chemistry, it is possible to adjust the pH at which the switching occurs. A method was developed for applying the new zwitterionic surface chemistry onto polyethersulfone (PES) ultrafiltration membranes. Bacteria deposition studies showed that the new chemistry performed better than other common anti-fouling chemistries. Biofilm studies showed that PES ultrafiltration membranes coated with the new chemistry accumulated half the biomass volume as unmodified membranes. Biofilm studies also showed that PES membranes coated with the new chemistry in the anti-microbial mode attained higher biofilm mortality than PES membranes coated with a common, non-switchable zwitterionic polymer.

Results from our research are expected to improve membrane performance for the purification of wastewaters prior to use in irrigation. Since reduction in flux due to biofouling is one of the largest costs associated with membrane processes in water treatment, using dual-mode nanolayer coatings that switch between passive and active control of biofouling and enable detachment of attached biofoulants would have significant economic and societal impacts.

Specifically, this research program developed and tested advanced ultrafiltration membranes for the treatment of wastewaters. Such membranes could find use in membrane bioreactors treating municipal wastewater, a slightly upgraded version of what presently is used in Israel for irrigation. They also may find use for pretreatment of agricultural wastewaters, e.g., rendering facility wastewater, prior to reverse osmosis for desalination. The need to desalinate such impaired waters water for unlimited agricultural use is likely in the near future.

Summary Sheet

Publication Summary

PubType	IS only	Joint	US only
Abstract - Poster	0	4	0
Abstract - Presentation	0	4	0
Other	0	0	1
Submitted	0	2	0

Training Summary

Trainee Type	Last Name	First Name	Institution	Country
Ph.D. Student	Weinman	Steven	Clemson University	USA
Postdoctoral Fellow	Bass	Maria	Technion	Israel
Postdoctoral Fellow	Kolev	Vesselin	Technion	Israel
Postdoctoral Fellow	Ying	Wang	Ben Gurion	Israel
Postdoctoral Fellow	Asa	Eli	Ben Gurion	Israel
Postdoctoral Fellow	Sweity	Amer	Ben Gurion	Israel

Contribution of Collaboration

The nature of the collaboration has been *synergistic*. The Husson group contributed expertise in monomer synthesis and surface-initiated polymerization, which enabled the dual-action coatings to be prepared on planar surfaces and membranes, with well-defined chemistry and structural properties. His group also contributed expertise in the characterization of these layers by various analytical tools, and performance testing of the membranes.

The Freger group contributed expertise in bacterial deposition on surfaces and membranes that the Husson group could not contribute and that was needed to understand the propensity for biofouling. Coated substrates and membranes prepared by Husson were sent to Freger for these tests. Freger also contributed expertise in concentration-enhanced polymerization and UV polymerization, two alternate membrane surface modification techniques, which allowed us to compare the performance of membranes prepared in different ways.

The Herzberg group contributed expertise in biofilm formation and characterization that could not be contributed by Husson or Freger, but that was needed to validate the antifouling and antimicrobial properties of the membranes. His group performed biofouling tests using membranes provided by Husson. The Herzberg group also contributed expertise in the use of quartz crystal microgravimetry (QCM), which enable real-time monitoring of bacterial attachment to the coatings prepared by Husson on QCM crystals.

During the course of the project, the team made numerous joint-effort presentations at conferences. To date we have delivered 3 presentations [1 invited] and 4 posters at conferences. A fourth presentation has been accepted for the 2017 American Institute of Chemical Engineers annual meeting, and a fifth was submitted as an invited paper for the 255 American Chemical Society National Meeting. In addition to these joint-effort presentations, we also submitted one joint-effort manuscript for publication to the Journal of Membrane Science, which is the premier journal in membrane science. A second joint-effort manuscript is under preparation but has not been submitted at the time of this report. One undergraduate student, Jacob Lass, completed his honors thesis on this project.

The team used Skype regularly to discuss results and plan research activities. In addition, we had several in-person meetings at conferences that included the 2014 and 2017 International Congress on Membranes, and the 2014 North American Membrane Society Meeting.

Achievements

This research project focused on knowledge generation to advance the development of membranes for the treatment of agricultural and municipal wastewaters, thereby addressing BARD's priority on *Water Quality & Quantity*. It introduced a novel membrane coating strategy to combat biofouling, which is a major problem for the membrane-based treatment of agricultural and municipal wastewaters. Results from our research are expected to improve membrane performance in the pretreatment of these wastewaters that require treatment for reuse in irrigation. Specifically, gained knowledge can be used to improve membrane design for purification of these impaired waters. Since reduction in flux due to biofouling is one of the largest costs associated with membrane processes in water treatment, implementation of the new coatings developed in this project could have significant economic and societal impacts.

The research had two complementary objectives: (1) prepare, characterize, and test dual-mode polymer nanolayers on planar surfaces and (2) evaluate these nanolayers as membrane modifiers for biofouling control. Attaining the first objective provided a fundamental understanding of how polymer nanolayer chemistry and structure impact bacterial deposition and removal, and how organic foulants can interfere with the anti-biofouling action of the nanolayers. Attaining the second objective required membrane development, characterization, and testing using model wastewaters. Below are the primary results and deliverables by the team related to the original objectives and associated tasks.

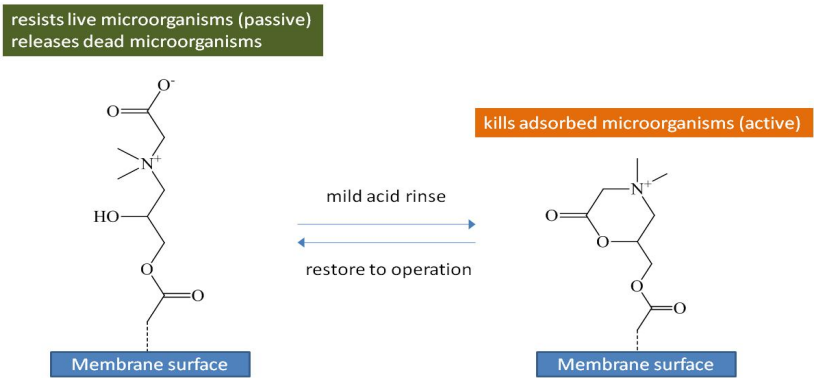

Significant results and deliverables of this research include:

- Method for the production of a new class of ultrafiltration membranes that couples passive and active biofouling control mechanisms in the treatment of agricultural and municipal wastewaters. This method applies one chemistry to a membrane surface that is capable of switching between a unique anti-fouling, carboxybetaine zwitterion mode (CBOH) and an anti-microbial, quaternary amine mode (CB-ring). The novelty of this chemistry is that it can

switch between the anti-fouling and the anti-microbial mode by changing the environment pH. This study is the first to apply switchable zwitterion chemistry to control membrane biofouling, and the first to study its effectiveness under long-term exposure to water. Polyethersulfone ultrafiltration membranes were modified with this chemistry and other anti-fouling chemistries to provide direct comparisons of the resistance to bacteria attachment, cell viability and biofilm growth on the membrane surfaces. These ultrafiltration membranes may find use in membrane bioreactors or as a pretreatment alternative prior to desalination by reverse osmosis.

- Data from performance testing that demonstrate that the coated membranes decrease the rate of bacterial attachment and biofilm formation relative to the best state-of-the-art membranes by presenting a passive (antifouling) surface. Poly(CBOH) modified polyethersulfone membranes had the lowest bacteria deposition coefficient among all membranes. The cause for the poly(CBOH) modified PES having the lowest bacteria deposition coefficient can be attributed to the increase in hydration upon immersion in water as well as the weaker hydrophobic interactions expected with bacteria as a result of a lower surface free energy, as measured using contact angle goniometry with two test fluids.

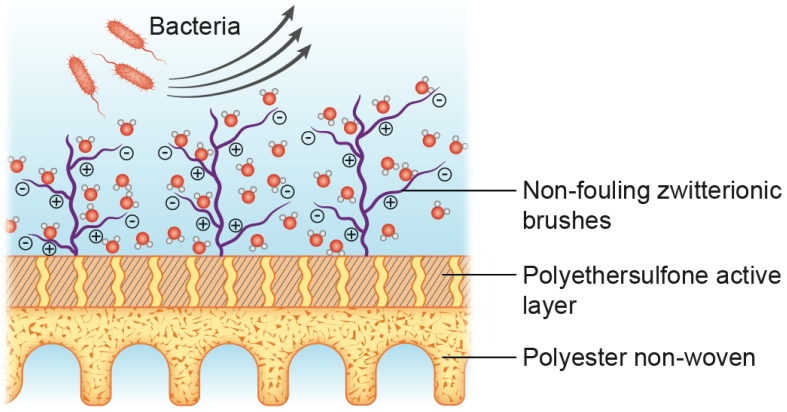

- Data from biofilm formation studies that demonstrate an increase in biofilm mortality by switching to an active (antimicrobial) surface using a simple acid rinse step.
- Fundamental studies on dual-mode nanolayer coatings that provide a deeper understanding of how the chemical and structural properties of these coatings impact the switching kinetics and the pH at which switching occurs. Results show that switching between passive and active modes is reversible for at least 50 cycles (the maximum number of cycles tested), which is important for enabling intermittent cleaning during long-term operation.
- Three new dual-mode monomers that switch between zwitterionic and quaternary amine chemistry at different pH values.

Near-term realization of societal and economic benefits (impact) from this research is expected by dissemination of the results *to potential users*. Thus, we have made a strong effort to network and deliver joint-effort presentations at a variety of conferences including meetings of the North American Membrane Society (NAMS), International Congress on Membranes and Membrane Processes (ICOM), American Institute of Chemical Engineers (AIChE), American Filtration Society (AFS), and American Chemical Society (ACS). We have submitted one joint-effort manuscript to the Journal of Membrane Science for publication, with a second under preparation.

This project has provided training and a research basis for postdoctoral researchers, one PhD student, and one honors undergraduate researcher. PhD student Steven Weinman has been recognized with several internationally competitive awards resulting from this work. He received a 2017 NAMS Student Fellowship Award, which is the most prestigious award given by this organization to only three students annually. He received 1st prize poster for membrane properties research at the 2015 NAMS meeting, 3rd place in the American Filtration Society Filtration and Separations in Power Generation Conference Student Poster competition, and Honorable mention in the American Filtration Society Filtration Clean Air and Water Solutions Conference Student Poster competition.

Development of water treatment/reuse technologies for the benefit of agriculture is of tremendous societal importance all around the world. In these applications, membrane exposure to feed waters containing biological and abiotic species leads to fouling and loss of membrane performance over time. There is tremendous potential for switchable membranes in these water treatment applications. The novelty of our concept is that we modify membrane surfaces with dual-mode nanolayers that switch reversibly between *passive* control during water treatment and *active* control during membrane cleaning. The intermittent use and relatively short time spent by the membrane in the active antimicrobial state may have additional advantages of minimizing adaptation of the microorganism to the specific surface-anchored biocide and preserving its activity for longer time. Using these switchable nanolayer coatings to limit and reverse membrane fouling is expected to improve the performance and lifetime of membranes for water purification in agricultural and other industries.

Changes to the Original Research Plan

We discovered early in the project that the switching pH of the zwitterionic nanolayers was much lower than anticipated, making it difficult to evaluate its antimicrobial effects. The solution pH conditions needed to switch to the antimicrobial state also kill the bacteria during long-term exposure. While we were able to demonstrate that the nanolayers were antimicrobial, we also decided to spend some time in Year 3 and during the no-cost extension to investigate the use of a different precursor during monomer synthesis. We showed that we could shift the switching pH to higher values by simple changes to the precursor chemistry.

Publications for Project US-4654-13

Status	Type	Authors	Title	Journal	Vol:pg Year	Coun
Published	Abstract - Poster	*Weinman, S.; Freger, V.; Herzberg, M.; Husson, S.M.*	Development of Anti-Fouling, Anti-Microbial Membranes for Wastewater Treatment	***Filtration and Separations in Power Generation Conference***	: 2015	Joint
Published	Abstract - Poster	*Weinman, S., Freger, V.; Herzberg, M.; Husson, S.M.*	Development of Anti-Fouling, Anti-Microbial Membranes for Wastewater Treatment	***2015 North American Membrane Society Meeting***	: 2015	Joint
Published	Other	*Perry, J.*	Dual-Mode Fouling Resistant Membranes for Water Purification	***Honors Thesis, Clemson University, Clemson SC, 2015***	: 2015	US only
Submitted	Reviewed	*Weinman, S.T.; Bass, M.; Pandit, S.; Herzberg, M.; Freger, V.; Husson, S.M.*	A switchable zwitterionic membrane surface chemistry for biofouling control	***Journal of Membrane Science***	: 2017	Joint
Published	Abstract - Poster	*Weinman, S.T.; Bass, M.; Freger, V.; Herzberg, M.; Husson, S.M.*	Development of Anti-Fouling, Anti-Microbial Membranes for Wastewater Treatment	***2016 North American Membrane Society Meeting, Seattle, WA***	: 2016	Joint
Published	Abstract - Presentation	*Weinman, S.T.; Bass, M.; Herzberg, M.; Freger, V.; Husson, S.M.*	Development of Anti-Fouling, Anti-Microbial Membranes for Wastewater Treatment	***2016 AIChE Annual Meeting, San Francisco, CA***	: 2016	Joint
Published	Abstract - Presentation	*Husson, S.M.; Weinman, S.T.; Duval, C.E.; Bass, M.; Darge, A.; Mannion, J.; Malakian, A.; DeVol, T.A.; Herzberg, M.; Freger, V.;*	Discovering membrane surfaces that promote or hinder binding	***Telluride Science Research Center Meeting on Molecular Engineering for Soft Matter***	: 2017	Joint
Submitted	Abstract - Presentation	*Weinman, S.T.; Bass, M.; Pandit, S.; Herzberg, M.; Freger, V.; Husson, S.M.*	A switchable zwitterionic membrane surface chemistry for biofouling control	***255th ACS National Meeting, New Orleans, LA,***	: 2018	Joint
Published	Abstract - Presentation	*Husson, S.M.; Weinman, S.T.; Bass, M.; Herzberg, M.; Freger, V.*	Patterned and switchable membranes for biofouling control	***11th International Congress on Membranes and Membrane Processes, San Francisco, CA***	: 2017	Joint
Published	Abstract - Poster	*Weinman, S.T.; Bass, M.; Herzberg, M.; Freger, V.; Husson, S.M.*	Application of a new zwitterionic membrane surface chemistry for biofouling control	***11th International Congress on Membranes and Membrane Processes, San***	: 2017	Joint

				Francisco, CA		
Accepted	Abstract - Presentation	*Weinman, S.T.; Bass, M.; Freger, V.; M.; Herzberg, Husson, S.M.*	Application of a new zwitterionic membrane surface chemistry for biofouling control	***2017 AIChE Annual Meeting, Minneapolis, MN, October 29-Nov 3, 2017***	: 2017	Joint

Appendix

Unpublished data briefly summarized

Monomer Synthesis. The first switchable monomer was synthesized according to the method proposed by Cao et al. [1] with slight alterations. A catalyst (zinc tetrafluoroborate hydrate) was used in an attempt to decrease the time and the temperature required for the amine-epoxide reaction [2]. Ten mole percent catalyst was used at 25°C for 24 hours, which is a reduction from 60°C and 60 hours. These conditions yielded 60-70 percent conversion. ^{1}HNMR and ^{13}CNMR were used to validate intermediate and final products. This monomer was sent to the Freger group at Technion for development of their graft polymerization methodology.

The second step of the monomer synthesis presented challenges because no clear formulation was proposed in Cao et al [1]. The formulation needed to be determined by experimental trials. We discovered that the mass and form of the ion-exchange resin was extremely important. If there was too much ion-exchange resin, the desired product was cleaved yielding unusable product. If the resin had too high of an –OH content, the desired product was also cleaved yielding an unusable product. Also, the final product after freeze-drying was not a white powder as described in Cao et al [1]. It is more of solid gel-like material, which is more consistent with expectations of freeze-drying.

The CB-OH monomer was verified to switch confirmation reversibly to the CB-Ring in solution. The switching of CB-OH to CB-Ring was demonstrated by dissolving CB-OH in TFA-d for 4 h and recording the NMR spectrum. Despite this initial success, a new synthesis protocol was developed to improve the yield and shorten the synthesis time period. The final protocol is presented in the submitted manuscript.

In addition to the original monomer synthesis, we prepared two alternative monomers. Tests with the CB-OH monomer found that the pH needed for switching to the antimicrobial CB-Ring form was lower than expected. This result frustrated initial attempts to characterize the antimicrobial potency of the CB-Ring nanolayer, since the solution pH conditions needed to switch from the CB-OH form to the CB-Ring form also kill the bacteria. Thus, in an effort to increase the switching pH of CB-OH to CB-Ring, we modified the monomer chemistry slightly. We plan to publish the results of this effort; however, at the time of this report submission the data are unpublished.

Briefly, the ring closure reaction requires protonation of the carboxylic acid group on the CB-OH molecule. We hypothesized that increasing the alkyl chain length between the quaternary amine and the carboxylic acid head group of the zwitterion may increase the pKa of switching to a value that we can study antimicrobial potency. The basis for this hypothesis is that the acid group on sarcosine has a pKa of 2.36; thus, a low pH is needed to fully protonate this acid group. Replacing sarcosine t-butyl ester in the first reaction step with an amino acid having a higher pKa value should shift the pH needed for protonating the acid group to a higher value. For example, γ-aminobutyric acid has a pKa of 4.23. Therefore, we used the same monomer synthesis procedure, but instead of using sarcosine *tert*-butyl ester, we used γ-aminobutyric acid *tert*-butyl ester to increase the alkyl chain length from one to three carbons between the quaternary amine and the carboxylic acid head group. We used solid-phase

synthesis to form the polymer directly on the substrate, starting with silicon wafers to facilitate characterization. Silicon wafers were first cleaned by piranha solution, then dip-coated with a poly(glycidyl methacrylate) solution to form a polymer layer of approximately 40 nm. Then both the sarcosine *tert*-butyl ester and the γ-aminobutyric acid *tert*-butyl ester were reacted with these PGMA coated wafers individually at 60 °C for 48 h. The *tert*-butyl group was then removed simply by immersion in phosphoric acid for 6 h. FTIR was used to study if the chemistry was successful and to test the switching behavior as a function of pH. The initial sarcosine based silicon wafers switched at a pH of 1.0. Figure 1 shows the transmission FTIR spectra of the γ-aminobutyric acid based silicon wafers in various solutions. The peak at approximately 1570 cm^{-1} for the "water" spectrum is assigned to the carboxylic acid group of γ-aminobutyric acid, which indicates successful attachment of γ-aminobutyric acid to PGMA. Interestingly, the carboxylic acid peak shifted from 1640 cm^{-1} for the sarcosine based silicon wafers to 1570 cm^{-1} for the γ-aminobutyric acid based silicon wafers. It was found that the γ-aminobutyric acid based silicon wafers switched at approximately pH 2.5 based on the peak shift from 1570 cm^{-1} to 1675 cm^{-1}. Discussion with the Freger group generated a question about whether the new chemistry would increase hydrophobicity of the coating, due to the increased alkyl chain length. Water contact angles were measured for samples prepared using the two modification chemistries. Figure 2 shows the water contact angle for the sarcosine based silicon wafers and the γ-aminobutyric acid based silicon wafers. It was found that there was no significant difference between the sarcosine based silicon wafers and the γ-aminobutyric acid based silicon wafers, thus alleviating concerns about increased hydrophobicity.

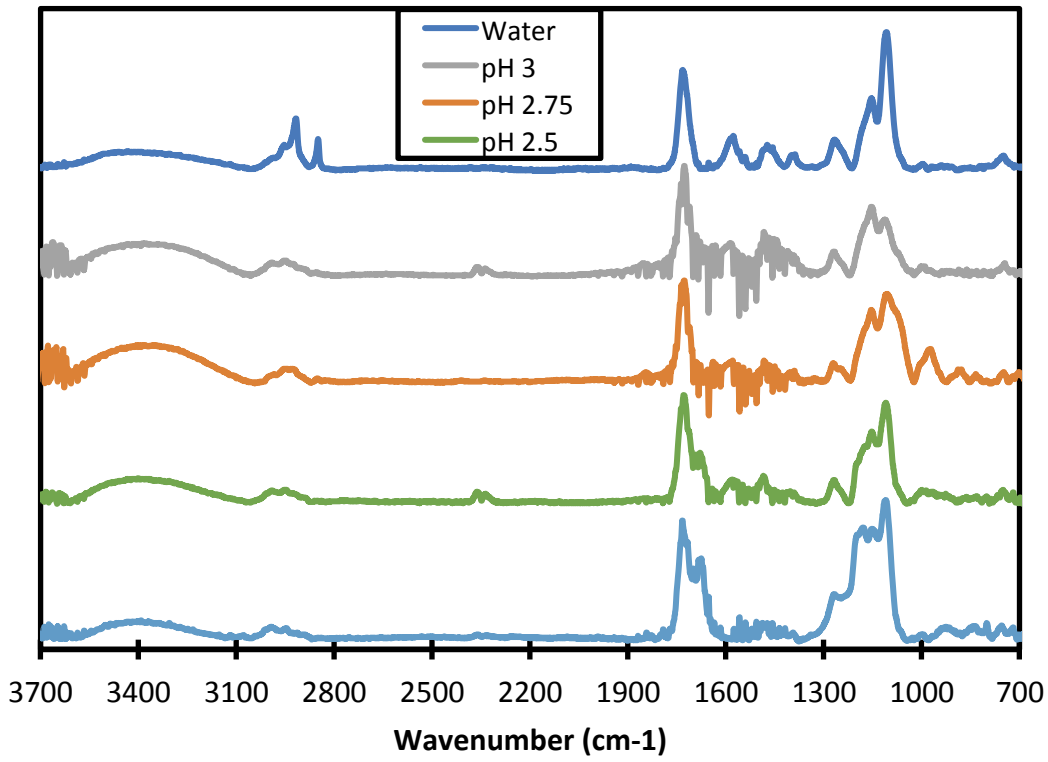

Figure 1. Transmission FTIR spectra of γ-aminobutyric acid based CBOH on silicon wafers exposed to varying pH solutions for 0.5 h. The CB-OH layer is approximately 40 nm thick.

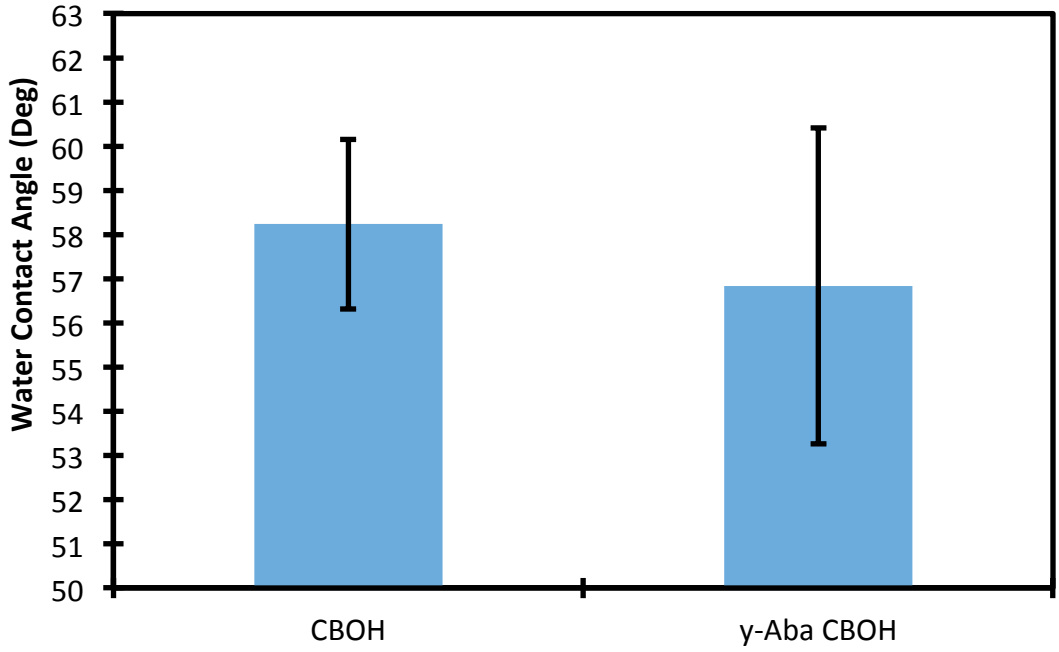

Figure 2. Water contact angle data for sarcosine based silicon wafers (CBOH) and γ-aminobutyric acid based silicon wafers (y-Aba CBOH). The error bars represent one standard deviation among at least 6 data points.

The pKa of the acid group on sarcosine (one methylene group between the amine and acid group) is 2.12, and the pKa of betaine (the quaternized amine version of sarcosine) is 1.83. Therefore, quaternization of the amine shifts the pKa of the carboxylic acid group by 0.4 units. We expect to see less impact on the acid pKa as the number of methylene groups increases between the quaternary amine and the carboxylic acid. The pKa of γ-aminobutyric acid is 4.23. Therefore one might expect the pKa to decrease to no lower than about 3.8 upon quaternization. Upon polymerization, it appears the effective pKa reduces an additional approximately 1-1.5 units (based on switching data in Figure 1). In an effort to further increase this pKa, a new monomer was ordered: *tert*-butyl 5-aminopentanoate. The pKa of pentanoic acid is 4.84, similar to that of butyric acid. The pKa upon adding the amine end group and further quaternization was expected to decrease to no more than 4.0 and upon polymerization to no more than 3.0. We found by experiment that the switching occurred between about pH 2.5 and 3.

***Polymer Nanolayer Preparation*.** Surface-initiated atom transfer radical polymerization (ATRP) was used to graft poly(CB-OH) nanolayers from silicon wafers and glass slides. The Freger and Herzberg groups used the glass slides for evaluation of microbial biofilm formation and adhesion of biofilm related components (bacteria and EPS). The silicon wafers were used to characterize the physicochemical properties of the polymer nanolayers and validate their ability to switch between antifouling and antimicrobial conformations.

The polymerization formulation was established to be 0.1M CB-OH, 0.1M Cu(I)Br, and 0.3M bpy in DMF:water (3:1 v/v). Ellipsometry was used to measure the polymer thickness. A multilayer model was created that included all the preparatory layers for the polymerization: SiO_2, poly(glycidyl methacrylate), and bromopropionic acid (initiator). The polymerization time was varied and the thickness measured by fitting

the ellipsometry data with the model. Figure 3 shows the results. A short polymerization time (1-3 hours) was satisfactory.

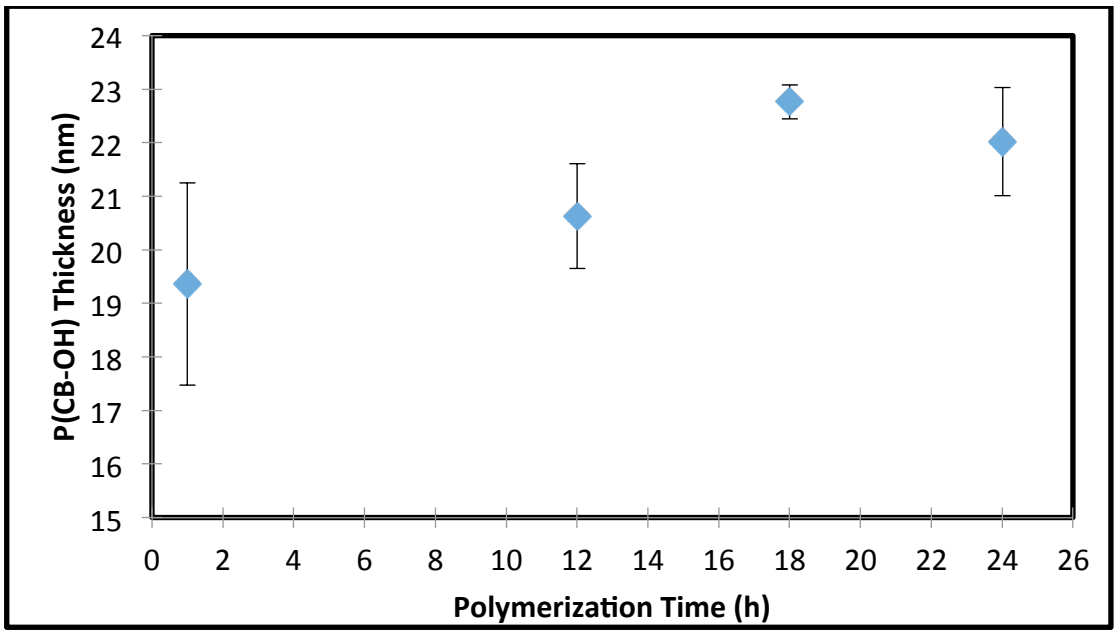

Figure 3. Thickness of CB-OH polymer (nm) versus polymerization time (h). CB-OH was grafted from PGMA-coated silicon wafers using ATRP. Error bars represent standard deviations among at least 3 measurements.

The silicon wafers modified with the CB-OH polymer were subjected to different pH solutions to determine the appropriate pH to achieve a high conversion of the CB-OH to the CB-Ring form that is needed to kill attached bacteria on the surface. Those results are published; however, we also studied the role of grafting density on the pH switching. Decrease grafting density had no noticeable effect on the switching pH from CB-OH to CB-Ring.

Validation of Adhesion of EPS Extracted from Biofilm. A procedure for analysis of adhesion of EPS in a QCM-D flow cell was developed in the Herzberg lab. The aim was to analyze the effect of the dual-mode polymer coatings on the interaction of the coated surface with microbial biofilm components, bacteria and their self-produced EPS. Modified QCM-D sensors with the dual-mode polymer were fabricated in the Husson lab. Figure 4 provides an example for adsorption of EPS onto polyamide-coated sensor and the effect of washing. In addition to the frequency shifts, indicative for mass adsorption and desorption to and from the quartz coated crystal, also dissipation factors were collected to enable analysis of changes in the viscoelastic properties and conformational changes of the fouling layers and the related effects of the passive and active mode of the polymer coating.

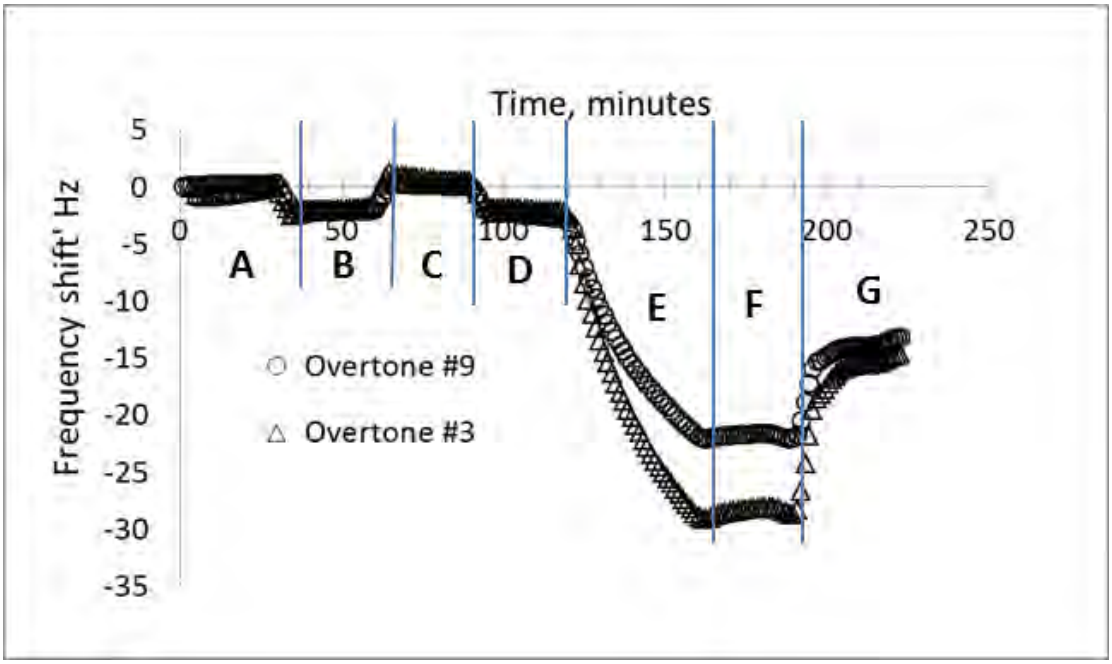

Figure 4. EPS (extracted from biofilm of *S. wittichii RW1*) adsorption kinetics to polyamide coated sensor analyzed as the frequency shift at different overtones (#3 – 15 MHz, #9 – 45 MHz): (A) baseline with DI water; (B) 100 mM NaCl; (C) DI water; (D) 100 mM NaCl; (E) 15 mg/L as DOC of EPS in 100 mM NaCl; (F) DI water.

Membrane development. One of the purposes of the project was to develop and test advanced reverse osmosis (RO) and nanofiltration (NF) membranes for treatment of agricultural wastewaters. A dual-mode zwitterionic polymer poly(carboxybetaine-OH methacrylate (poly(CB-OH)) was studied in the project as a material that potentially could be used for preparation of anti-(bio)fouling nanolayers on polyamide (PA) membranes surfaces. This monomer was synthesized by the Husson group and shipped to the Freger group to perform grafting experiments. Preliminary grafting tests were performed along with commercially-available 2-(methacryloyloxy)ethyl] dimethyl-(3-sulfopropyl) ammonium hydroxide (SPE) as a reference.

Commercial desalination membranes were surface-modified by radical graft polymerization using concentration-polarization (CP) enhanced grafting method. Attenuated Total Reflection FTIR (ATR-FTIR) was used to verify the presence of the modification polymer on membranes surfaces. The extent of grafting was quantified using a degree of grafting (GD) that was calculated as $GD=A_{1725}/A_{1586}$, where A_{1725} is the area of the 1725cm^{-1} IR band of the carbonyl group, characteristic of the grafted polymer and A_{1586} was the area of the 1585 cm^{-1} IR band characteristic of the base membrane (polysulfone support). Figure 5 displays typical ATR-FTIR spectra of a pristine and SPE-modified NF-270 membrane, showing the characteristic bands of the SPE polymer. The carbonyl band at 1725 cm^{-1} and 1040 cm^{-1} band assigned to the sulfonate group clearly appear in the spectra of the modified samples.

However, during the work we found that grafting of hydrophilic zwitterions on PA surface is more challenging than grafting of hydrophobic monomers, successfully grafted on PA membranes in the past [3,4]. Wide variety of modification conditions,

i.e. monomer/cross-linker ratio, monomer concentration, initiation method, reaction time etc. were tested with two different PA membranes, semi-aromatic NF-270 and fully aromatic ESPA-1. Unfortunately, no clear effects of the tested factors on the resulted grafting were observed and the overall grafting degrees were very low (Figure 6). The additional tests conducted after washing the samples at the elevated temperature (60 °C) showed that most of the modification polymer had been washed away, whatever modification conditions were used. This suggests that the obtained modification layers were mostly physically attached to the membranes surface and not chemically grafted. This was markedly different from experiments where grafted polymer was not water-soluble and could adhere to the surface. For instance, a significant and stable grafting was obtained for NF-270 and ESPA-1 membranes modified with hydroxyethyl methacrylate (HEMA), forming a mildly hydrophilic yet water-insoluble polymer, using the same modification conditions (Figure 7 a,b).

Scanning Electron Microscopy (SEM) examination of ESPA-1 membrane surface modified with SPE and HEMA polymers strengthened the view that a physical attachment of modification polymers to PA surface could be mainly responsible for obtaining coating layers by modification, thereby more hydrophobic HEMA polymer covered the PA surface much better than hydrophilic poly-zwitterion. Figure 8 shows SEM images of the pristine and the surface-modified ESPA-1 samples. Figures 8a and b show the surfaces of HEMA-modified membranes that were presumably coated with either thick (1.5 microns) or a thin (24 nm) layer of poly(HEMA). (The average thickness was deduced form respective GDs, 5.6 and 0.08, using the method of reference [5]). Figure 8c shows the surface of ESPA-1 with a small grafting by poly(SPE) (4 nm, GD=0.06), which looks fairly similar to pristine ESPA-1 (Figure 8d). The SEM images demonstrate that on all modified membranes there remained large uncovered surface areas, even though the total amounts of the coating polymer could vary greatly.

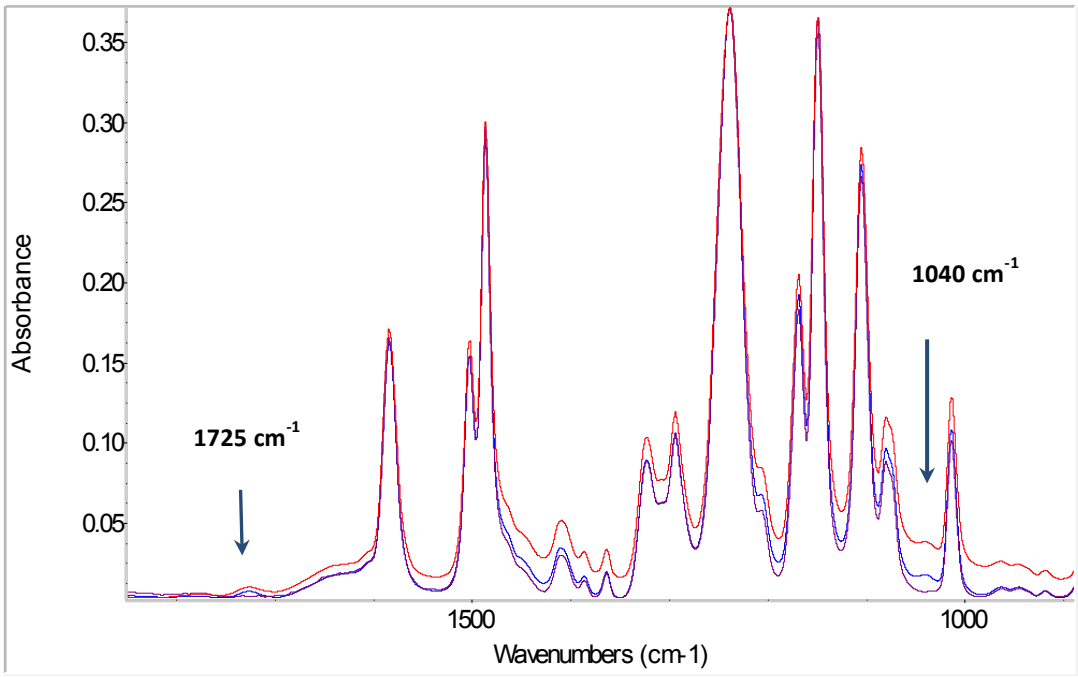

Figure 5. ATR-FTIR spectra of a pristine (purple) and poly(SPE)-modified (red and blue) NF-270 membranes.

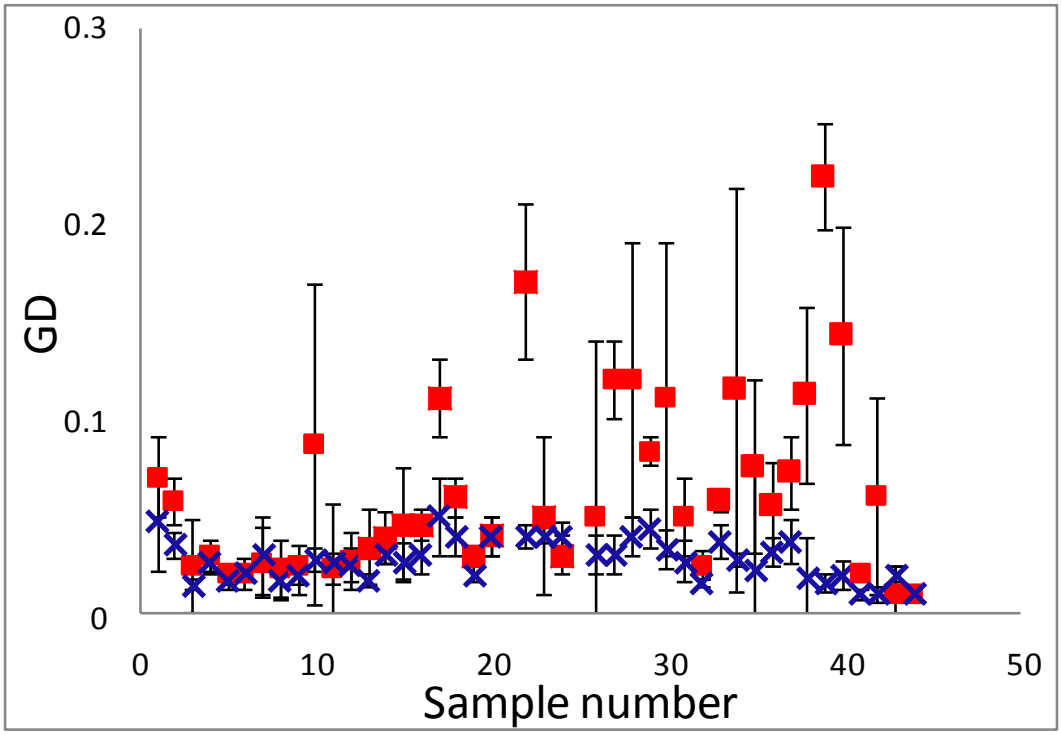

Figure 6. Grafting degrees measured for a number of NF-270 membrane samples modified with polySPE by CPE graft polymerization using various modification conditions. The varied parameters were monomer amount, initiators amounts, % of cross-linker, reaction time, pH of the modification solution. Squares - room temperature wash, X – 60C wash.

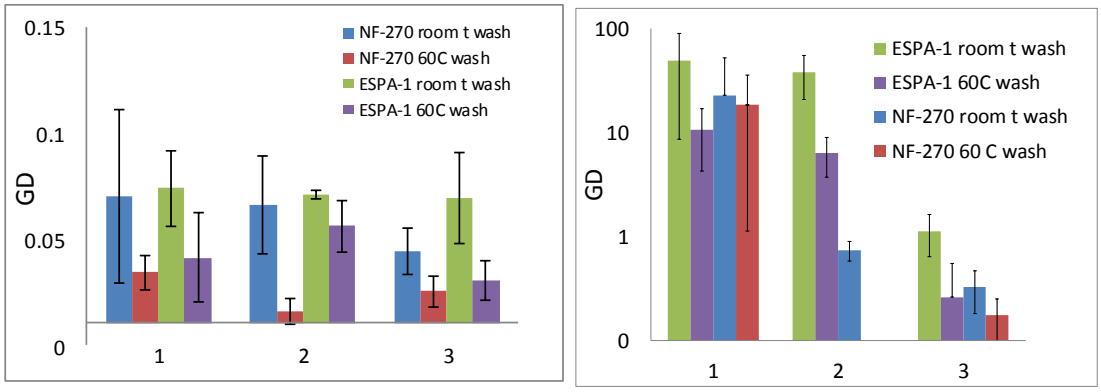

(a) (b)

Figure 7. The extent of grafting measured for SPE-modified (a) and HEMA-modified (b) NF-270 and ESPA-1 membranes after room and elevated temperature wash using various initiation conditions: 1-APS 4mM/TEMED 2mM, 2-$K_2S_2O_8$ 4mM/$K_2S_2O_5$ 2mM, 3–APS 4mM/TEMED 8mM.

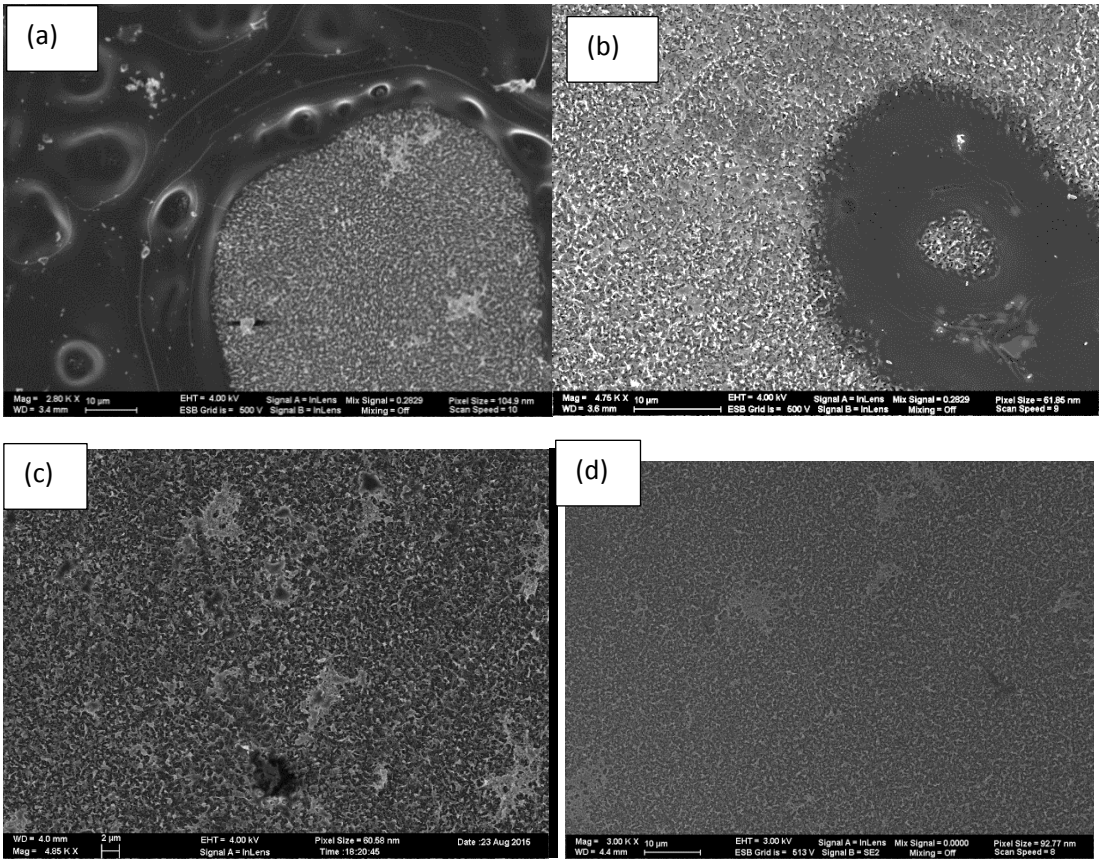

Figure 8. SEM images of HEMA-modified (GD= 0.08) (a), of HEMA-modified (GD= 5.6) (b), SPE-modified (GD= 0.06) (c) and pristine ESPA-1 membrane (d).

To clarify whether the difficulty of obtaining continuous and stable modification layers was related to the use of CP-enhanced grafting based on chemical redox initiation, modified membranes was also prepared using UV-assisted radical grafting of polySPE on ESPA-1. A high GD (GD≈1.2) was measured for the samples after short wash at room temperature, but the coating was again non-uniform. SEM images of the modified membranes clearly showed that UV-assisted grafting resulted in formation of polymer aggregates deposited on the polyamide surface rather than in a homogeneous polySPE layer (Figure 9). This result confirmed the assumption that weak physical interactions of polySPE with polyamide could be the reason for poor grafting. This also suggests that zwitterionic nature and hydrophilicity of polySPE might prevent homogeneous grafting, since zwitterionic groups tend to segregate on the hydrophobic membrane surface, driven by their strong polarity and dipole-dipole interactions [6]. As a result they may tend to form clusters or small fragments rather than uniformly adhere to the surface. It also agrees with the results by Shkolnik and Behar who observed that grafting of sulfonate monomers onto polyethylene was not feasible due to the lack of compatibility between highly hydrophilic sulfonate groups and the hydrophobic polymer carrying the radical sites was the reason [7].

Based on the above results, we concluded that new modification methods should be found and tested for grafting zwitterionic SPE and CB-OH monomers on PA membranes. (An attempt to graft CB-OH monomer on PA membrane using redox-

initiated CP enhanced grafting was also done; the obtained GD was immeasurably low). It should be noted that non-continuous coatings could still be beneficial for "plugging" small defects in PA and so for improving rejection of poor-rejected substances [8]. In this respect, it was reported that commercial polyamide membranes containing a coating layer may also display heterogeneous surface composition, indicative of the presence both coated and uncoated surfaces [9-11]. The imperfect coating may then also beneficial for increasing fouling resistance. However, well-defined and uniform modification would be clearly preferred for successful and reliable long-term use for reducing biofouling. We then continued to seek and test other approaches for improving the uniformity and stability of zwitterionic layers grafted on PA membranes.

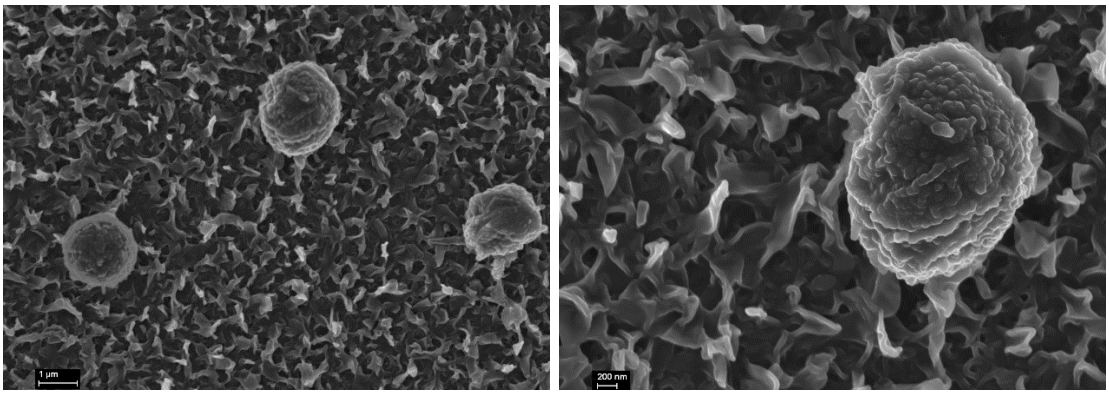

Figure 9. SEM images of ESPA-1 membrane modified by UV assisted grafting of 0.3M of SPE with the addition of 3% (mol) cross linker (MBAA).

For instance, we tried to combine "grafting from" and "grafting to" procedures. The modified membranes were tested with a number of surface analysis techniques (ATR-FTIR, Atomic Force Microscopy, Low Vacuum Scanning Electron Microscopy, Time-of –Flight Secondary Ion Mass Spectroscopy). Unfortunately, the method did not show a systematic improvement of the grafted layer uniformity. Other tested methods included additional modification steps and employed materials that should help to anchor zwitterionic polymers covalently to the membrane surface. Best results were obtained using two-steps grafting procedure, where in the first step thin poly-glycidyl methacrylate (polyGMA) layer was grafted on PA and then polySPE was anchored to it by the regular concentration-polarization (CP) enhanced grafting method at a slightly elevated temperature (40 °C). Figure 10 shows grafting degrees measured for ESPA-1 membrane samples modified using both this procedure and the regular CP enhanced grafting; GD of the membranes modified by GMA only also shown for comparison, because the carbonyl band that was used for GD determination characteristic for GMA layers as well. The results shown for all three samples were obtained after washing the modified membranes at 60 °C. It is clearly seen that polySPE layer remained on the membrane even after it was washed at the elevated temperature. SEM observation of the samples confirmed that uniform modification layers of polySPE were obtained (Figure 11). Unfortunately, the developed procedure was not tested for CB-OH polymer since its amount was very limited and insufficient for modifying even a few ESPA-1 membrane samples.

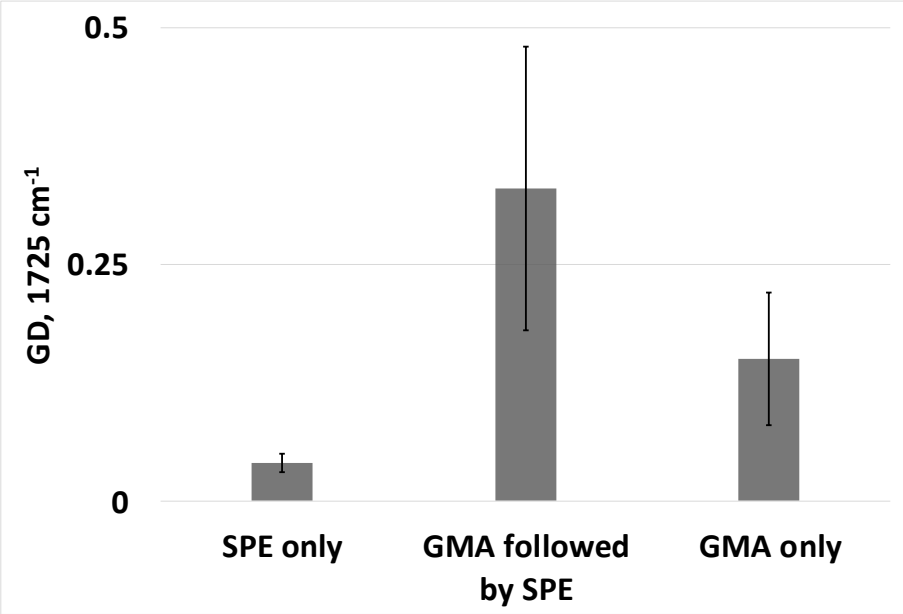

Figure 10. Grafting degrees measured for ESPA-1 membrane modified with polySPE, polyGMA and with the both monomers by the two-steps procedure, where SPE was grafted after GMA. All samples were tested after washing at an elevated (60 °C) temperature.

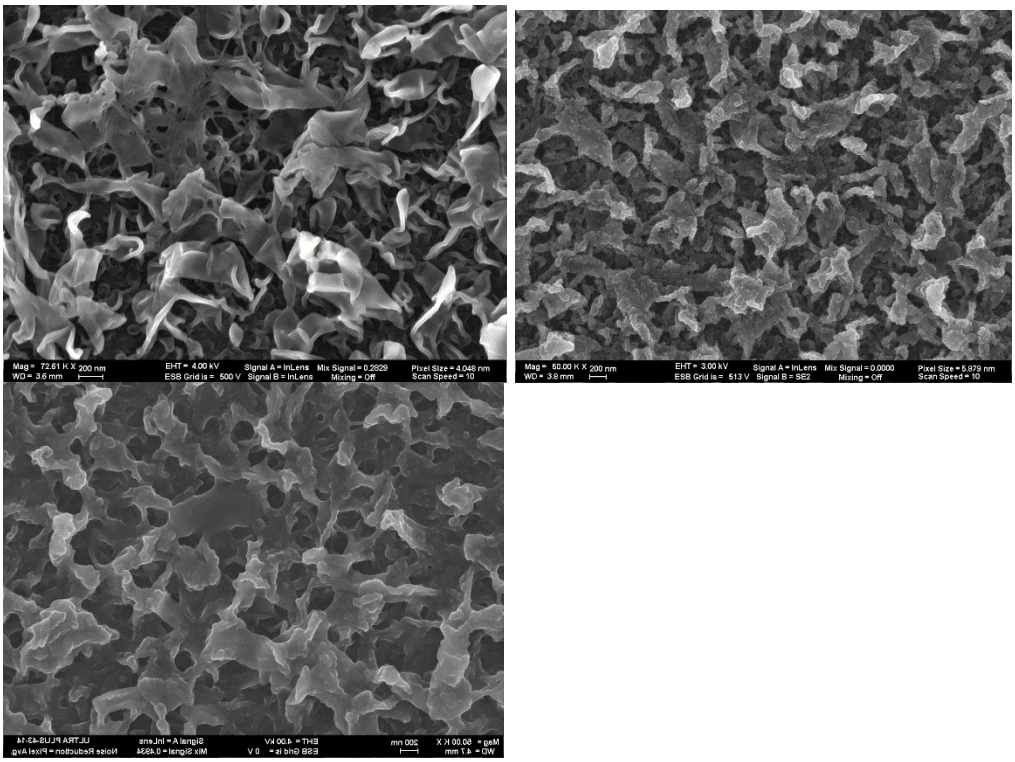

Figure 11. SEM images of ESPA-1 pristine (a), ESPA-1 modified by polyGMA (with the addition of Triton) (b) and ESPA-1 modified using the two-steps procedure, where poly SPE layer was grafted on polyGMA-modified membrane. The samples were imaged after the elevated (60 °C) temperature wash.

Fouling resistance of CB-OH polymer. It was demonstrated that coating PES membranes with thin layers of poly(CB-OH) decreases membrane propensity to initial bacteria deposition and biofouling [12]. Ion addition, we tested its effect on organic fouling, which is another factor that seriously reduces membranes flux and restricts the types of water that suits for desalination treatment for irrigation [13]. Notably, adsorption of organic materials on membrane surface increases its propensity to bacteria attachment and, then, to biofouling, i.e., there is a synergy between the two types of fouling [14, 15]. It was then presumed that the resistance of CB-OH polymer layers to organic fouling would be important for wastewater treatment.

Organic fouling resistance of CB-OH polymer was evaluated using QCM with Dissipation (QCM-D). QCM enables to measure very small changes in the mass adsorbed to the surface by measuring the changes in the frequency of quartz crystal. Monitoring of dissipation gives information about the mechanical properties of the adsorbed layers. First, we intended to prepare QCMD crystals coated with a pristine membrane material (polysulfone (PS)) and then graft the modification polymers (poly(CB-OH), (poly(SPE) and poly(PEGMA)) on PS-coated sensors via UV-assisted grafting. The fouling propensity was supposed to be measured by testing the adsorption of model fouling materials on the prepared surfaces.

The modification procedure was first tested using Si wafers, whose oxidized silica surface is similar to QCMD sensors used. Pieces of a Si wafer were cleaned and spin-coated with polysulfone (PS) using 0.6% (w) PS solution in dichloromethane (DCM). Ellipsometry showed that the layers with a reproducible thickness of 63±2 nm were obtained. The modification procedure used for PES membranes modification with poly(CB-OH) was not suitable for QCMD crystal since it included soaking the samples in organic solution (100mM BPh in acetonitrile) that could damage the crystals. PS is a photosensitive material that can be activated without a photoinitiator, however using photoinitiator can increase the obtained GD at certain irradiation conditions [16]. To obtain a measurable GD of poly(CB-OH) without BPh, we irradiated the samples without using a glass filter, that increased the irradiation intensity and the range of irradiation wavelengths. (This method did not suit PS membranes since the irradiation of PS with the wavelengths lower than 300 nm damages it and deteriorates membrane performance [16,17].) FTIR tests showed that the samples were successfully modified with all tested polymers, although the degree of modifications was low. Unfortunately, the same procedure applied to QCMD sensors damaged the sensors' Au electrodes layers, therefore the fouling tests could not be carried out as planned.

However, an assessment of fouling propensity of CB-OH polymer was done by measuring its affinity to gold QCMD sensors and comparing it with gold affinity of poly(PEGMA) and poly(SPE). When handled in a lab air atmosphere, gold QCMD sensors are relatively hydrophobic (CA= 65°) even after plasma cleaning, since less than a monolayer contamination of gold makes it hydrophobic [18]. So low affinity of a polymer to a gold crystal could be seen as an indication of its low-fouling properties. The polymer solutions were prepared by redox polymerization of 0.5M monomers solutions contained 1% (mole) of a cross-linker (MBAA). Ammonium persulfate (APS, 0.04M) and tetramethylethylenediamine (TEMED, 0.02M) were used to initiate the polymerization reactions. The solutions were stirred for about five minutes after adding the initiators to monomer/MBAA solution, and then left

overnight on Vortex shaker. In addition, a solution contained just APS and TEMED was prepared in order to evaluate the response of QCMD crystal to these materials.

In the QCMD tests stable baselines were obtained with DDW and then the prepared solutions were fed for 30 min (polySPE and polyPEGMA) or for 35 min (poly(CB-OH) and APS/TEMED), then the feed solutions were again replaced with DDW. Figure 12 shows the real-time recording of obtained frequency changes, where overtones 3,5, and 7 are displayed for each sample. The affinity of the polymers to the gold sensors was evaluated by the comparison of the masses (layers thicknesses) that stayed on the crystals after the feed solution was changed to DDW. The layers thicknesses were calculated using the Voigt viscoelastic model, the analysis was done using QTools software for the frequency and the dissipation data measured for each sensor for 3,5 and 7 overtones. Table 1 summarizes the obtained results. It was found that the affinity of poly(CB-OH) to a hydrophobic surface was lower than those of poly(SPE) and poly(PEGMA), that makes this material an attractive candidate for preparing low-fouling membranes by surface-modification of commercial desalination membranes.

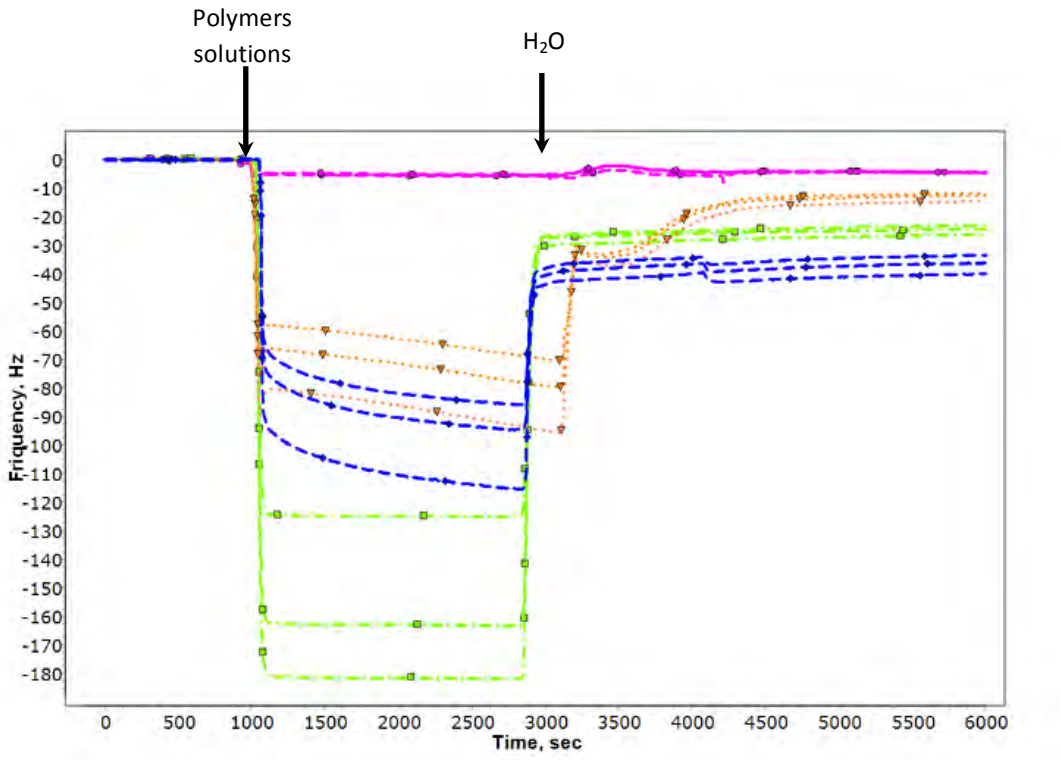

Figure 12. The real-time recording of the frequency changes during polymers layers deposition, overtones 3, 5 and 7 shown for each sample. Green-poly(PEGMA), blue-poly(SPE), orange – poly(CB-OH). Magenta lines show the response of a gold crystal to APS/TEMED solution. *(The solutions of poly(CB-OH) and APS/TEMED were fed to QCMD 5 min longer than poly(SPE) and poly(CB-OH).*

Table 1. Density and thicknesses of the polymers layers built on gold QCMD crystals.

Polymer	Layer density, kg/m^3	Layer thickness, mm
CB-OH	1.025	2.4
PEGMA	1.006	4.24
SPE	1.024	6.04

Hollow Fiber Membranes. In addition to work with flat-sheet membranes, the Herzberg group carried out preliminary work on surface modification by graft-polymerization from UF membranes made from polyvinylidene fluoride (PVDF). A hollow fiber UF PVDF membrane was graft-polymerized using different monomers and tested for its fouling propensity with soluble microbial products (SMP) of a membrane bioreactor treating municipal wastewater of Sede-Boqer campus in BGU. The PVDF-based hollow fiber membranes by GE-Zenon were cut from actual hollow fiber modules and were tested in the UF-MBR system. Commercially available acrylic monomers with various functionalities including PEGMA, zwitterionic SPE, negatively charged SPM (including a cross linker MBAA), and co-polymerization with SPM and MOETMA. For graft polymerization of the monomers from the surface we used redox couples as initiators: a mixture of persulfate and metabisulfite, which were mixed in situ immediately before the grafting reaction. In the case of UF membrane surface, specificity is poor, but good contact between the reactants and membrane including membrane pores was achieved by filtration of the monomers and initiators through the membrane during the graft-polymerization as shown in Figure 13.

The UF fiber was modified by redox-initiated graft polymerization performed in aqueous solution at room temperature. UF membrane PVDF fibers were cut from ZW-10 hollow fiber module (Zenon, GE). Two different modification procedures were used to modify pristine fibers, in triplicate for each procedure. The fibers were first washed by filtering double distilled water (DDW) until a stable flow rate baseline was acquired. Thereafter, an aqueous solution containing monomers (as mentioned above, at a concentration of 0.5 M) and a solution of initiators, potassium persulfate (0.02 M; $K_2S_2O_8$) and potassium metabisulfite (0.02 M; $K_2S_2O_5$), were simultaneously injected into the system under flow rate of 4 ml/min from each vessel (see Figure 13). Two different hydraulic modes of injecting the reactants to the system were implemented, differently affecting the grafting process. In the "bypass" mode, the reactants were pumped along the outside surface of the fiber with the bypass valve fully open, i.e., without exerting any significant trans-membrane pressure difference resulting in a negligible permeate flow. In the "filtration" mode a pressure of 0.7 bar was applied across the membrane by partially closing the bypass valve (Figure 13). Grafting process was terminated after permeate flux declined by 20-30%, which took 20 to 270 min, and immediately afterwards the module was flushed with DDW to terminate grafting and filtration of the DDW through the membrane fiber was continued for 2 h. Figure 14 shows the result of flux decline experiments using the modified hollow fiber membranes.

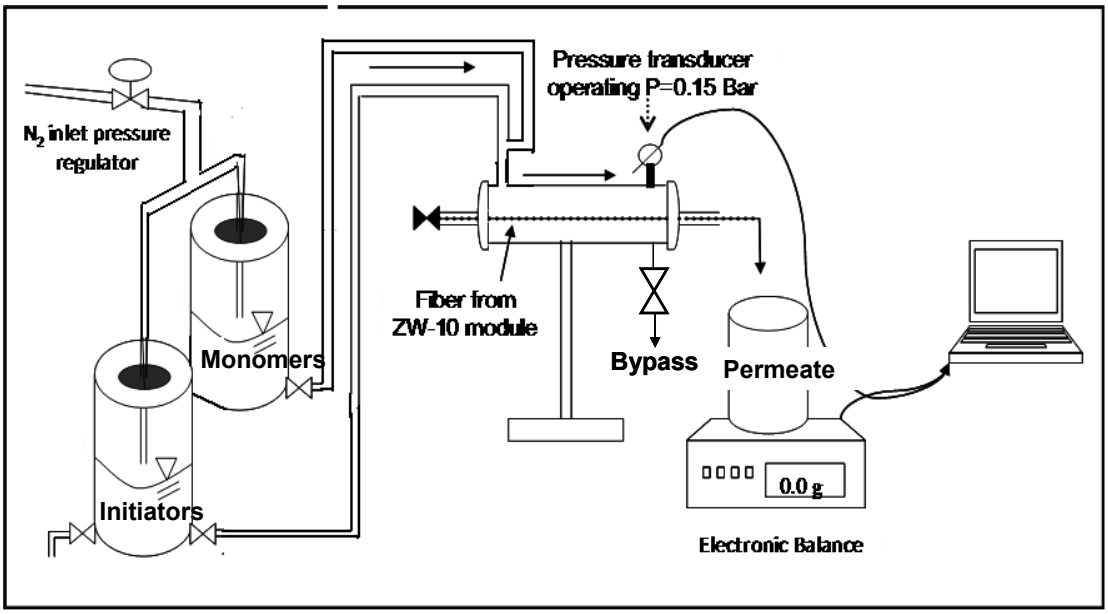

Figure 13. Schematic representation of a setup for modifying single UF membrane fibers including two 1-liter tanks for solutions of initiators and monomers, 100 ml tubular housing for grafting a single outside-in fiber, an electronic balance for monitoring permeate flow and pressure transducers.

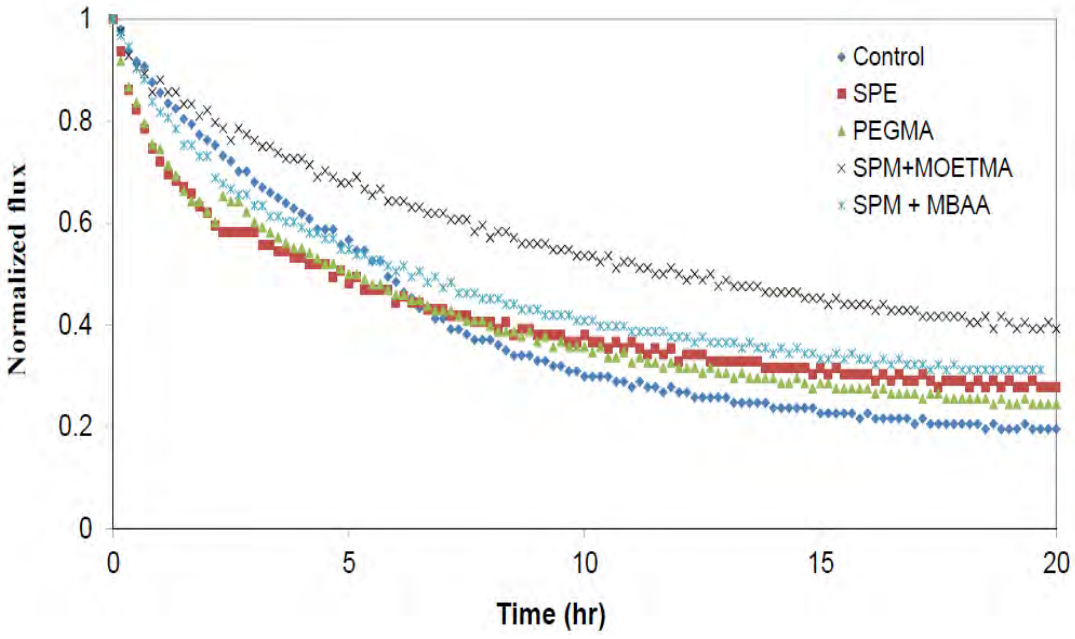

Figure 14. Enhanced permeate flux decline during filtration of SMP solution, extracted from aerobic MBR at concentration and diluted to 10 mg/L as TOC. Initial membrane permeabilities was 0.2 ± 0.03 $cm \cdot min^{-1} \cdot bar^{-1}$ and the permeate flow rate was similar for all fibers (1 $mL \cdot min^{-1}$).

References

[1] Z. Cao, N. Bault, H. Xue, A. Keefe, S. Jiang, *Angew. Chem. Int. Ed.* **2011**, *50*, 6102.

[2] B. Pujala, S. Rana, A. Chakraborti, *J. Org. Chem.* **2011**, *76*, 8768.

[3] R. Bernstein, S. Belfer and V. Freger, *Langmuir,* (2010) 26(14) 12358-12365.

[4] S. Belfer et al., *J. Membr. Sci.*, (1998) 139 175-181.

[5] M. Bass, V. Freger, *J. Membr. Sci.*, (2015) 492 348-354.

[6] P. Bengani, Y. Kou, A. Asatekin, *J. Membr. Sci.*, (2015) 493 755-765.

[7] S. Shkolnik, D. Behar, *J. Appl. Polym. Sci.*, (1982) 27 2189-2196.

[8] A. Ben-David, R. Bernstein, Y. Oran, S. Belfer, C. Dozoretz, V. Freger, *J. Membr. Sci.*, (2010) 357 (1-2) 152-159.

[9] C.Y. Tang, Y.N. Kwon, J.O. Leckie, *J. Membr. Sci.* 287 (2007) 146–156.

[10] C. Wang, G. K. Such, A. Widjaya, H. Lomas, G. Stevens, F. Caruso, S. E. Kentish., *J. Membr. Sci.* 409 (2012) 9-15.

[11] A. Widjaya, T. Hoang, G. W. Stevens, S. E. Kentish, *Sep. Purif. Technol.* 89 (2012): 270-281.

[12] S. Weinman, M. Bass, M. Herzberg, V. Freger, S. M. Husson*, J. Memb. Sci.*, submitted

[13] G-D. Kang, Y-M. Cao, *Water research*, (2012) 46 584-600.

[14] R. Donlan, *Emerging Infectious Diseases* (2002) 8 (9) 881-889.

[15] Y. Baek, J. Yu, S-H Kim, S. Lee, J. Yoon*, J. Membr. Sci.*, (2011) 382 91-99.

[16] M. Ulbricht, M. Riedel, U. Marx, *J. Membr. Sci.*, (1996) 120 239-259.

[17] J.P. James, V. Crivello, G. Belfort, *Chem. Mater.*, (2002) 14 256-265.

[18] T. Smith, *Journal of Colloid and Interface Science*, (1980) 75(1) 51-55.

A switchable zwitterionic membrane surface chemistry for biofouling control

Steven T. Weinman,[†] Maria Bass,[§] Soumya Pandit, [‡] Moshe Herzberg,[‡] Viatcheslav Freger,[§] Scott M. Husson[*,†]

[†]Department of Chemical and Biomolecular Engineering, Clemson University, Clemson, SC 29634, USA

[§]Wolfson Department of Chemical Engineering, Technion - Israel Institute of Technology, Haifa, 32000 Israel

[‡]Zuckerberg Institute for Water Research, Ben Gurion University of the Negev, Sede-Boqer Campus, Midreshet Ben Gurion, 84990 Israel

*Corresponding author: Tel: +1 (864)-656-4502, Fax: +1 (864)-656-0784. Email address: shusson@clemson.edu

Abstract

This contribution describes a method to minimize biofouling of ultrafiltration membranes by coating the membrane surfaces with a new type of zwitterionic polymer. Poly(2-((2-hydroxy-3-(methacryloyloxy)propyl)dimethylammonio)acetate) (poly(CBOH)) was grafted from polyethersulfone (PES) membranes by UV-photopolymerization. Bacteria deposition studies showed that the poly(CBOH) chemistry performed better than other common anti-fouling chemistries. Biofilm studies showed that poly(CBOH) functionalized PES membranes accumulated half the biovolume as unmodified membranes. A unique feature of this new polymer coating is that it can switch reversibly between the anti-fouling, zwitterion mode and an anti-microbial, quaternary amine mode. Switching pH and time needed for complete switching to occur were evaluated using poly(CBOH) functionalized silicon wafers. Switching pH was

determined to be 1.0, with 15 min being required to switch between the zwitterion and quaternary amine chemistries. Biofilm mortality was elevated once the anti-fouling poly(CBOH) zwitterion was switched to the anti-microbial, poly(CB-Ring) quaternary amine, with dead-to-live cell ratio increasing from 0.33 to 1.04.

Keywords: Anti-fouling; Anti-microbial; Carboxybetaine; pH responsive; Surface modification; Ultrafiltration membrane; Water treatment

1. Introduction

Membrane biofouling is a process involving the adsorption of biopolymers, such as glycoproteins and polysaccharides, to the membrane surface; attachment of microorganisms, such as bacteria and algae, to the biopolymer conditioning layer; and eventually growth of the microorganisms into a fully developed biofilm on the membrane surface [1]. Biofouling is a major hindrance to membrane usage, because unlike other types of fouling, microorganisms can grow, multiply, and relocate on a membrane [2]. Biofouling causes a transient flux decline in the case of constant-pressure filtration or a pressure increase in the case of constant flux filtration, either of which increases the process operational costs [3]. Chemical cleaning is required for fouled membranes, which leads to process downtime and shortens the membrane lifetime [4].

Biofouling prevention not surprisingly has been a trending topic in the literature. Surface modification of membrane surfaces has been the most common approach to reducing biofouling, and typically is done by chemical treatments or coatings [5]. Anti-fouling coatings make the membrane surface less favorable for biopolymer/bacteria attachment by following the

"Whitesides' rules": making the surface more hydrophilic, including hydrogen-bond acceptors, excluding hydrogen-bond donors, and having an overall neutral electrical charge [6]. Commonly studied anti-fouling coatings include poly(ethylene glycol) (PEG) [7, 8] and zwitterions such as carboxybetaine [9], sulfobetaine [10, 11], and phosphobetaine [12], which are net charge neutral molecules that contain positive and negative charge groups. These coating types can form a strong hydration layer that decreases biofoulant adsorption or attachment [7, 13]. Recently, we showed that membrane biofouling resistance can be enhanced by combining chemical surface modification with physical surface modification using a nano-scale line and groove pattern [14].

Application of anti-microbial agents or biocides is another common strategy used to control membrane biofouling by killing bacteria that attach to the surface. Quaternary amine containing coatings are thought to disrupt the cell membrane, resulting in cell leakage and eventually cell death [15]. Carbon nanotubes and graphene oxide have been shown to deactivate the bacteria upon contact with the membrane surface [16]. Silver nanoparticles that severely damage the bacteria cell membrane also have been incorporated in membranes [17].

There have been attempts to combine anti-fouling and anti-microbial approaches on one membrane [18]. One strategy has been to use an anti-fouling chemistry combined with silver nanoparticles [19]. A second strategy has been to add two chemistries to the membrane surface, one anti-fouling and the other anti-microbial [20, 21]. One such method is to pattern the two chemistries on the membrane in alternating rows of a stimuli-responsive polymer and a biocide, such that foulants will be brought in contact with the biocide, killed, and released by the stimuli responsive polymer [21].

This paper contributes a method for applying one chemistry to a membrane surface that is capable of switching between a unique anti-fouling, carboxybetaine zwitterion mode and an anti-

microbial, quaternary amine mode [22, 23]. The novelty of this chemistry is that it can switch between the anti-fouling and the anti-microbial mode by changing the environment pH. Similar zwitterion chemistries with switching capabilities have been studied as hydrogels [24]. This study is the first to apply a switchable zwitterion chemistry to control membrane biofouling, and the first to study its effectiveness under long-term exposure to water. Polyethersulfone ultrafiltration membranes were modified with this chemistry and other anti-fouling chemistries to provide direct comparisons of the resistance to bacteria attachment, cell viability, and biofilm growth on the membrane surfaces.

2. Materials and Methods

2.1. Materials

All chemicals were used as received, unless otherwise noted. The following chemicals were purchased from Sigma Aldrich: sarcosine *tert*-butyl ester hydrochloride (97%), glycidyl methacrylate (GMA, 97%), zinc tetrafluoroborate hydrate, iodomethane (99%), trifluoroacetic acid (TFA, 99+%), Amberlite® IRA-400 chloride form, N,N-dimethylformamide (DMF, anhydrous, 99.8%), [2-(methacryloyloxy)ethyl]dimethyl-(3-sulfopropyl)ammonium hydroxide (SPE, 97%), benzophenone (BP, 99%), N,N'-methylenebis(acrylamide) (MBAA, 99%), poly(ethylene glycol) methacrylate (PEGMA, M_n = 360 g/mol), 2-bromo-2-methylpropionic acid (BPA, 98%), copper (I) bromide (99.999%), 2,2'-bipyridyl (BPY, 99+%), chloroform-d (99.8%), deuterium oxide (99.9%), trifluoroacetic acid-d (99.5%), azobisisobutyronitrile (AIBN, 98%), hydrogen peroxide (30% in water), and sulfuric acid (95-98%). The following chemicals were purchased from Acros Organics: chloroform (99%), dichloromethane (DCM, pure), diethyl ether (99.5%), and diiodomethane (99+%). Acetone (99.5+%), sodium bicarbonate (99+%),

tetrahydrofuran (THF, 99+%), and acetonitrile (anhydrous, 99.9%) were purchased from Fisher Scientific. Sodium hydroxide (97+%) was purchased from Alfa Aesar. Aqueous solutions were made with deionized water from a Milli-Q water purification system (Millipore-Sigma).

Prior to reaction, GMA was passed through a column of inhibitor remover (Sigma Aldrich) to remove monomethyl ether hydroquinone. Anhydrous DMF was opened and was stored in a nitrogen atmosphere glovebox (MBraun USA). Poly(glycidyl methacrylate) (PGMA, MW = 290,000 g/mol, PDI = 1.7 (GPC)) [25] used for dip-coating silicon wafers was prepared by radical polymerization of GMA in methyl ethyl ketone at 60°C using AIBN as initiator. Amberlite® IRA-400 chloride form was converted to hydroxide form by reacting with a 1 M sodium hydroxide aqueous solution using a 1 meq resin:2 mmol sodium hydroxide stoichiometry for 35 min.

PES ultrafiltration membranes were kindly received from Microdyn-Nadir GmbH (PM UP150, Microdyn-Nadir) and GE Water & Process Technologies (GE Osmonics). The GE PES membrane was a gift from GE. Polished silicon wafers (1 cm × 3 cm) were purchased from Nova Electronic Materials.

The synthesis of the carboxybetaine zwitterion monomer (CBOH) is presented in supporting information in two parts: (1) synthesis of the protected monomer (CBtBu) and (2) deprotection to yield the final product. The steps are similar to those reported by Cao et al. [22], but with modifications. Experimental details (Figure S3) and ^{1}H- and ^{13}C-NMR spectra (Figures S4 and S5) are given in the supporting information.

2.2. Surface Modification

2.2.1. UV polymerization

UV polymerization was performed to graft poly(CBOH), poly(PEGMA), and poly(SPE)

from PES ultrafiltration membranes. Figure S2 in the supporting information depicts the process for polymerizing poly(CBOH) from PES membranes. PES membranes were rinsed in deionized water to remove pore filler and pat dried. Photo-initiator, BP, was entrapped in PES membranes by immersing the PES membranes in a solution of 100 mM BP in acetonitrile for 4 h with stirring. Acetonitrile was chosen because it swelled but did not dissolve the PES. The PES membranes were rinsed thoroughly with deionized water to collapse the swollen PES to entrap the BP and then pat dried. Next, UV polymerization was performed using a 365 nm UV light from an EL series UVLS-28 UV lamp (UVP, VWR International) (Husson lab) or a 315-600 nm range UV lamp (UVACUBE100 curing chamber equipped with Dr. Hönle lamp UV 150F and filter H1 (Hönle UV technology)) (Freger lab).

Modification of Microdyn-Nadir PM UP150 PES membranes by poly(CBOH) and poly(SPE) was done in the Husson lab at Clemson University. The reaction solution comprised 1 M CBOH or SPE and 0.01 M MBAA in deionized water. A piece of BP-entrapped PES membrane was placed in a 50 mL glass beaker and 0.17 mL of reaction solution/cm^2 membrane area was placed on the membrane active side. A 30 mL glass beaker was placed on top of the membrane and the reaction solution such that no air bubbles were present between the membrane and the top glass beaker. For flux and dextran rejection experiments, a glass petri-dish was used instead of beakers, with the membrane being placed in the top cover of petri-dish and the bottom part used to form the thin film of reaction solution. The membrane was exposed to 365 nm UV light with an intensity of at least 500 $\mu W/cm^2$ for 4.5 h (CBOH) or 25 min (SPE) from a source placed approximately 6.5 cm above the membrane. Modified membranes were rinsed thoroughly with deionized water, placed in deionized water in a shaker bath overnight (>15 h), and then pat dried. Samples for ATR-FTIR were vacuum dried at 20-25 °C and -0.78 to -0.95 barg. Samples

for biofilm studies were immersed in a 15 wt% aqueous glycerol solution and dried in air for shipment to the Herzberg lab at Ben Gurion University.

Modification of GE Osmonics PES membranes was done in the Freger lab at Technion. The following protocol was used for poly(CBOH), poly(SPE), and poly(PEGMA) UV polymerizations. First, BP was entrapped in PES membrane samples as described earlier in this section. Then a piece of the membrane was placed in the cover of a glass Petri dish, 5 mL of a monomer/cross-linker solution in DI water (0.5M monomer, 0.005M MBAA) was put on top of the membrane, and the bottom part of the Petri dish turned upside down was placed on the membrane. This procedure produces a thin layer of the modification solution on top of the membrane between the two glass Petri dish components. The assembly was placed in the UV chamber (UVACUBE 100, Hönle UV technology) and UV-irradiated for 5 min (SPE and PEGMA monomers) or 10 min (CBOH monomer). The modified membranes were rinsed with DI water, washed with shaking in DI water overnight and stored in fresh DI water. A piece of each sample was dried at 30 °C for ATR-FTIR tests.

2.2.2. ATRP

Atom transfer radical polymerization (ATRP) was performed to graft poly(CBOH) from silicon wafers substrates (Figure S1). Silicon wafer substrate preparation was similar to that reported by Bhut et al. [26], with minor modifications. Silicon wafer substrate cleaning procedure and experimental details on the grafting procedure can be found in the supporting information. PGMA was deposited onto the clean silicon wafer substrates from a 0.5 wt% PGMA solution in chloroform using a dip coater (QPI-128, Qualtech Products Industry Co. LTD) at an immersion and withdrawal rate of 60 mm/min. PGMA-coated silicon wafer substrates were annealed at

110 °C for 30 min under vacuum (-0.78 to -0.95 barg) to react some of the epoxy groups of PGMA to silanol groups on the silicon wafer substrate surface. BPA was reacted to the remaining epoxy groups of PGMA from the vapor phase at low pressure (-0.78 to -0.95 barg) and 100 °C for at least 18 h to form α-bromoester initiator groups on the silicon wafer substrate surface. After BPA reaction, the silicon wafer substrates were washed thoroughly with THF and deionized water and dried. Deionized water used for ATRP was de-oxygenated by three cycles of freeze–pump–thaw and transferred to the glove box.

Poly(CBOH) was grown from initiator-functionalized silicon wafer substrates by surface-initiated ATRP similar to Cao et al. [22], but with minor modifications. An initiator-functionalized silicon wafer substrate was placed into the reaction mixture comprising copper (I) bromide (0.1 M), BPY (0.3 M), and CBOH monomer (0.1 M) in a 3:1 (v/v) mixture of DMF and deionized water inside the glovebox. Polymerization was done at 35 °C for 3 h. Polymerization was terminated by removing the silicon wafer substrates from the reaction mixture and washing thoroughly with a 3:1 (v/v) DMF and deionized water mixture.

2.3. Characterization techniques

2.3.1. ATR-FTIR Spectroscopy

Attenuated total reflectance Fourier-transform infrared spectroscopy (ATR-FTIR) was used to characterize the surface chemistry of the unmodified and chemically modified PES membranes. Measurements at Clemson University were done using a Thermo Scientific Nicolet iS50R FT-IR with an ATR accessory (Specac Golden Gate) equipped with a diamond ATR crystal. Data were processed by OMNIC 9.3.32 software. Each spectrum was collected from 128 scans at a resolution of 4 cm^{-1} corrected with the ATR software, and manually baseline

corrected. A background of the ATR crystal was taken before each set of samples was tested. Measurements at Technion were done using a Nicolet 8700 FT-IR spectrometer (Thermo Electron Corporation) with an ATR accessory (Smart MIRacle accessory, Pike). Each spectrum was collected from 64 scans at a resolution of 4 cm^{-1}, at least 5 different places were tested on each sample, and the data were processed using OMNIC software.

2.3.2. FTIR Spectroscopy

Transmission Fourier-transform infrared spectroscopy (FTIR) was used to characterize the change in surface chemistry of the silicon wafers. Spectra were obtained using a Thermo Scientific Nicolet iS50R FT-IR. Data were processed by OMNIC 9.3.32 software (Thermo Scientific). Each spectrum was collected from 256 scans at a resolution of 4 cm^{-1}, and was manually baseline corrected. A background of an unmodified silicon wafer was taken before each set of samples was tested.

2.3.3. Static Contact Angle Goniometry

Water and diiodomethane contact angles were measured on silicon wafers to evaluate changes in hydrophilicity and surface free energy (SFE) associated with the changes in surface chemistry. All static contact angles were measured using a Krüss DSA 10-Mk2 contact angle goniometer. A liquid drop (~ 3.0 μL) was placed carefully on the sample surface. The sessile drop model was used in DSA version 1.80.0.2 Drop Shape Analysis software to determine contact angle. For consistency, measurements were taken 60 s after each droplet was placed on the surface. Measurements were done at a minimum of three locations on each sample to get an average contact angle value with standard deviation. SFE was calculated using the Owens-Wendt

method [27]. Equation details and constants used are presented in the supporting information.

2.4. Substrate performance testing

2.4.1. Water permeance testing of membranes

Water permeance was measured for the unmodified and surface modified PES membranes. Unmodified, BP entrapped, poly(CBOH) modified, poly(SPE) modified, and poly(PEGMA) modified GE PES membranes were tested at Technion in 165 mL cylindrical stainless steel direct-flow cell with an active membrane area of 11.3 cm^2 (diameter 38 mm) [28]. The cells were stirred magnetically and pressurized with nitrogen. The flux was determined at feed pressure of 3 bar by collecting and weighing the permeate.

Unmodified, BP entrapped, poly(CBOH), and poly(SPE) modified Microdyn-Nadir PES membranes were tested in direct-flow mode using a stainless steel Sterlitech HP4750 stirred cell with an active membrane area of 14.6 cm^2 at Clemson University. The cell was filled with approximately 280 mL of deionized water and pressurized to the desired pressure (up to 1.9 barg) with air (UN1002, Airgas). Each membrane was conditioned before making the flux measurement by passing at least 150 mL of water or running for 30 min, whichever came first. At least 8 g of permeate was collected while recording the time to collect that sample. At least 4 membranes were tested for each membrane type for statistical relevance.

2.4.2. Bacteria deposition studies on membranes

Pseudomonas fluorescens bacteria tagged with green fluorescent protein (GFP) were pre-cultured by incubating at 30 °C in Luria-Bertani (LB) broth (Sigma-Aldrich) in the presence of

25 μg/mL Kanamycin (Sigma-Aldrich) for 24 h. Then a 0.5 mL aliquot was transferred to fresh LB broth solution that also contained 25 μg/mL Kanamycin, and cultured for another 5 h. The cultured bacteria in the stationary stage of growth were centrifuged out, washed by suspending/centrifuging in 0.01 M NaCl (Sigma-Aldrich) solution three times, and finally suspended in a fresh 0.01 M NaCl solution and diluted to an optical density of 0.1 (bulk concentration $C_b = 2.99 \times 10^7 \pm 6 \times 10^6$ bacteria/cm^3). The experiments were carried out in a parallel plate flow cell setup (FC 81 flow cell, BioSurface Technologies) at room temperature. A glass slide with a 2.5 cm long piece of membrane glued on it was mounted inside the cell, forming the bottom of the channel. The bacterial suspension was fed to the cell at a flow rate of 2.0 mL/min, which corresponds to cross-flow velocity of 7.7 cm/min and shear rate of 230 min^{-1}. The bacteria deposited on the membrane surface were imaged and counted using a fluorescence microscope (Nikon LV100) equipped with a 20x objective lens and a digital camera. The imaged area was 0.148 mm^2 and was located in the middle of the cell. Images were taken every 5 min for 30-40 min. The mass transfer (deposition) coefficient k_d was calculated by Equation 1 assuming first-order deposition kinetics [11]:

$$k_d = \frac{1}{C_b A}\frac{dN}{dt} \quad (1)$$

N is the number of bacteria in the image, A is the imaged area, and C_b is the bacteria concentration in the feed solution. The reported k_d values are averages of at least 3 tests performed for each sample type, each time using a fresh bacteria suspension.

2.4.3. Switching between CBOH and CB-Ring

CBOH (monomer or polymer) has the ability to switch from the anti-fouling, zwitterion mode to the anti-microbial, quaternary amine mode (coined CB-Ring). Figure 1 depicts the

switching and Cao et al. [23] proposed the mechanism of reversible switching between CBOH and CB-Ring.

FTIR was used to study the switching of poly(CBOH) to poly(CB-Ring) and vice versa on silicon wafers. To switch from poly(CBOH) to poly(CB-Ring), the poly(CBOH) modified silicon wafers were placed in pure TFA for 1 h. To switch from poly(CB-Ring) to poly(CBOH), the poly(CB-Ring) modified silicon wafers were placed in deionized water for 1 h. To test the longevity of switching, a poly(CBOH) modified silicon wafer was placed in pure TFA for at least 0.33 h to switch to poly(CB-Ring), then the poly(CB-Ring) modified silicon wafer was placed in deionized water for at least 0.33 h to switch back to poly(CB-OH). This cyclical process was repeated 50 times, with FTIR spectra taken after 1, 10, and 50 cycles.

To test the pH at which the switching occurs, poly(CBOH) modified silicon wafers were immersed in TFA/water solutions with pH values of 0.6, 1.0, and 1.5 for 1 h with pH measured using an accumet Basic AB15 pH meter (Fisher Scientific) equipped with an accumet 13-620-285 pH probe (Fisher Scientific). To test the time needed for complete switching to occur from poly(CBOH) to poly(CB-Ring), the poly(CBOH) modified silicon wafers were placed in a TFA/water solution at pH 1.0 for 0-30 min. To test the time needed for complete switching to occur from poly(CB-Ring) to poly(CBOH), poly(CBOH) modified silicon wafers were placed in a pure TFA solution for 1 h to ensure complete conversion to poly(CB-Ring). Next they were placed in deionized water for 0-30 min.

2.4.4. Biofilm studies on membranes

Biofilm studies on PES membranes were conducted with *Sphingomonas wittichii* RW1 (GenBank #NC 00951), which was obtained from the DSMZ (Deutsche Sammlung von

Mikroorganismen and Zellkulturen GmbH) culture collection, Germany. The bacterium was grown on nutrient agar medium containing peptone (5 g/L) and meat extract (3 g/L) adjusted to pH 7 and supplemented with 150 µg/mL streptomycin (Sigma Aldrich, S6501). A single colony was inoculated overnight in 5 mL of the nutrient medium in a shaker–incubator at 150 rpm at 30 °C (ZHWY-1102C, ZHWY). Thereafter, the *S. wittichii* RW1 cells were diluted in the nutrient medium (1:100) and incubated for 24 h to achieve early stationary growth phase. Bacteria were harvested by centrifugation (4K15, Sigma) (4000g and 4 °C for 10 min) and the pellet was washed three times in fresh nutrient broth. After the washing steps, the optical density (OD_{600}) of the suspension was adjusted to 0.5 in wastewater effluents taken from MBR UF permeate, treating municipal wastewater of Sede Boqer BGU campus [29] and supplemented with 12.5 mg/L peptone and 7.5 mg/L meat extract. Twenty-five milliliters of the bacterial suspension were injected into the biofilm growth chamber, which was previously loaded with 5 mm × 5 mm membranes fixed on glass cover slips, at flow rate of 2 mL/min, as previously reported by Bernstein et al. [30]. *S.wittichii* RW1 biofilm was grown on the membranes for 4 d before sampling of the membrane coupons. Note that the conditions used for biofilm growth were very aggressive to keep the time period for experiments to a reasonable length. The membrane pieces with biofilm were carefully removed and stained with concanavalinA (ConA) conjugated to Alexa Fluor 633 (Invitrogen, Israel), SYTO 9, and propidium iodide (PI) for probing EPS, live cells, and dead cells with a confocal laser scanning microscope (CLSM). Probing EPS, live cells, and dead cells of the biofilms was carried out before and after rinsing poly(CBOH) modified and poly(SPE) modified Microdyn-Nadir PES membranes with 0.1 M HCl (pH 1) for 20 min.

Microscopic observation and image acquisition were performed using Zeiss-Meta510, a CLSM equipped with Zeiss dry objective LCI Plan-Neofluar (20x magnification and numerical

aperture of 0.5). The CLSM was equipped with detectors and filter sets for monitoring Alexa Fluor 633 bonded to ConA, SYTO 9, and PI stained cells (excitation wavelengths of 633, 568 and 488 nm, respectively). CLSM images were generated using the Zeiss LSM Image Browser. Images were analyzed, and the specific biovolume per membrane area ($\mu m^3/\mu m^2$), average thickness (μm) and roughness coefficient [31] of the biofilm layer were determined by COMSTAT [32], an image processing software written as a script in MatLab 6.5 (The Math Works, Inc., Natick, MA) and equipped with an image-processing tool box. For every sample, five to six positions on the membrane were chosen and microscopically observed, acquired, and analyzed. Three-dimensional reconstruction of the CLSM image stacks was carried out using Imaris software (Imaris Bitplane, Zurich, Switzerland).

3. Results and Discussion

3.1. PES membrane surface modification

Polyethersulfone membranes were surface modified using UV-graft polymerization. Even though polyethersulfone is UV active by itself [33], initial work found that the polymerization rate of CBOH from unmodified PES membranes was slow. Therefore, benzophenone (BP) photo-initiator was entrapped in the PES membranes to increase the polymerization rate and chain density by increasing the number of reaction sites on the PES membranes [34]. Figure 2 shows the ATR-FTIR spectra of GE (A) and Microdyn-Nadir PM UP150 (B) PES membranes surface modified with various chemistries. Both PES membranes showed successful BP entrapping by the presence of its characteristic carbonyl stretching peak centered at about 1655 cm^{-1} (as indicated by the arrows on the right side in Figure 2). There is a

slight evolution of a peak at about 1720 cm^{-1} in the polymer modified membrane spectrum (as indicated by arrows on the left side in Figure 2), which would correspond to carbonyl stretching of the grafted polymer layer. The small carbonyl stretching peak at about 1720 cm^{-1} indicates a very thin grafting layer of each polymer.

3.2. Water permeance of membranes

Water permeance of the modified PES membranes was measured to ensure the membrane was not plugged during surface modification. Figure 3 shows the water permeability coefficient versus the modified PES membrane type. Figure 3A shows the results for the GE PES membranes. The unmodified GE PES had an average water permeance of 123 $L/m^2/h/bar$. The modified membranes had a statistically significant lower water permeance than the unmodified GE PES. The BP entrapped GE PES had an average water permeance of 65 $L/m^2/h/bar$. This permeance reduction could be attributed to possible pore collapse due to the PES swelling in acetonitrile and subsequent collapse in water [35]. Poly(CBOH) modified, poly(SPE) modified, and poly(PEGMA) modified GE PES had average water permeances of 53, 31, and 26 $L/m^2/h/bar$ respectively. The further decrease in water permeance could be from increased resistance due to the grafted polymer layer on the surfaces (as described in section 3.1).

Figure 3B shows the results for the Microdyn-Nadir PES membranes. The unmodified PES had an average water permeance of 915 $L/m^2/h/bar$, which is similar to what has been reported in the literature [36]. The BP entrapped PES had an average water permeance of 503 $L/m^2/h/bar$, the poly(SPE) modified PES had an average water permeance of 22 $L/m^2/h/bar$, and the poly(CBOH) modified PES had an average water permeance of 770 $L/m^2/h/bar$. The error bars seem to indicate that the BP entrapped PES have a lower water permeance than the

unmodified PES; however, a multiple mean hypothesis test shows that only the poly(SPE) modified Microdyn-Nadir PES was statistically different from the 3 other membrane types at 95% confidence. (All statistical analysis details are given in the supplementary information.) The decrease in water permeance in the poly(SPE) modified PES could be from increased resistance due to the grafted polymer layer on the surfaces (as described in section 3.1).

3.3. Bacteria deposition on membranes

Bacteria deposition studies were performed on the surface-modified GE Osmonics PES membranes. GFP-tagged *Pseudomonas fluorescens* bacteria were injected parallel to the surface-modified PES membranes under conditions of no permeate flow and the number of bacteria adsorbed onto each membrane was counted as a function of time. The purpose of this study was to see how different surface modifications affected the bacteria interactions (adsorption characteristics) with the PES membranes. Table 1 shows the bacteria deposition coefficients that were calculated from Equation 1 for each membrane type. As expected, unmodified PES had a higher bacteria deposition coefficient of 1.4 μm/min due to the hydrophobic nature of the unmodified GE PES membranes (70° water contact angle [Figure S7 in supporting information]). Even with a very thin surface modification layer on the PES (as described in section 3.1), the bacteria deposition coefficient was reduced by approximately an order of magnitude with all modification types. Interestingly, the water contact angle of the dry polymer modified surfaces did not change much (only poly(PEGMA) modified PES had a statistically significant lower water contact angle [Figure S7]), suggesting hydration of the grafted polymer layers upon immersion in water plays a more important role than hydrophilicity of the membrane surface, as indicated by water contact angle values. Poly(PEGMA) modified PES had the highest bacteria

deposition coefficient of the modification layers with a value of 0.18 μm/min. Poly(SPE) modified PES had the next lowest bacteria deposition coefficient of 0.13 μm/min. Poly(CBOH) modified PES had the lowest bacteria deposition coefficient of 0.10 μm/min. The cause for the poly(CBOH) modified PES having the lowest bacteria deposition coefficient can be attributed to the increase in hydration upon immersion in water as well as the weaker hydrophobic interactions expected with bacteria as a result of a lower surface free energy as described in section 3.5. However statistically, all three modification layers on PES can be considered the same using a multiple mean hypothesis test (95% confidence). By this same test, all three are statistically different from the unmodified PES. These data show that even a thin modification layer could reduce the frequency of membrane cleanings.

3.4. Switching characteristics of poly(CBOH)

A unique feature of CBOH (monomer or polymer) is that it can switch reversibly between the anti-fouling, zwitterion mode (CBOH) and an anti-microbial, quaternary amine mode (CB-Ring). NMR was used to show that the CBOH monomer switches to the CB-Ring, as described in the supporting information (Figure S6). Fundamental studies were done using silicon wafer substrates to assess the polymer switching characteristics. Silicon wafers were chosen for this phase of the work to enable characterization of layer thicknesses by ellipsometry and to determine the switching pH and switching time without the concern of membrane degradation in low pH environments. CBOH was polymerized from silicon wafers using the graft-from ATRP method. FTIR was used to track the changes in surface chemistry. Poly(CBOH) layer thickness on silicon wafers was measured by ellipsometry as described in the supporting information.

3.4.1 Demonstration of polymer switching

Figure 4 shows the spectra demonstrating the successful grafting of poly(CBOH), successful switching to poly(CB-Ring), and successful switching back to poly(CBOH). The main peaks of interest to see the changes in surface chemistry are those from 1600 to 1800 cm^{-1} assigned to carbonyl stretching and those from 1150 to 1200 cm^{-1} assigned to C-O stretching. The peak at 1730 cm^{-1} in the BPA-modified spectrum is assigned to carbonyl stretching in PGMA and BPA. After poly(CBOH) grafting, the same peak at 1730 cm^{-1} increases in intensity, which corresponds to carbonyl stretching in the ester group next to the carbon backbone of the polymer. The new peak at 1640 cm^{-1} corresponds to the carboxylate anion of the poly(CBOH) zwitterion, indicating successful grafting of CBOH from the silicon wafers. Interestingly, the CBOH carboxylate anion peak shifted from 1705 cm^{-1} on PES membranes to 1640 cm^{-1} on silicon wafers. To test if the poly(CBOH) zwitterion switched to poly(CB-Ring), the poly(CBOH) modified silicon wafers were placed in pure TFA. The shift in the carbonyl stretching peak from 1640 cm^{-1} to 1680 cm^{-1} indicates a successful switch from poly(CBOH) to poly(CB-Ring). Also, the large increase in peak area at approximately 1150 cm^{-1} to 1200 cm^{-1} (assigned to C-O stretching) further supports successful switching from the carboxylate anion of poly(CBOH) (weak C-O stretching) to the acetate ester of poly(CB-Ring) (strong C-O stretching) [37]. The poly(CB-Ring) modified wafers were then placed in water to switch back to poly(CBOH). The spectrum for poly(CBOH) was fully recovered, indicating that switching was reversible.

3.4.2 Determination of switching pH

Poly(CBOH) modified silicon wafers were placed in solutions of various pH values for 1

h to study poly(CBOH) switching to poly(CB-Ring). As described by Cao et al. [23], the first step in the switching mechanism is protonation of the carboxylate anion, which requires a decrease in pH. Therefore the solution pH was decreased from pH 7 in 0.5 increments until switching was observed by FTIR. Figure 5 shows the FTIR spectra of the poly(CBOH) modified silicon wafers after immersion in deionized water, pure TFA, and TFA/water solutions at pH values of 0.6, 1, and 1.5 for 1 h. Switching started to occur at pH 1.5, however there was incomplete switching, as indicated by the presence of peaks at 1680 cm^{-1} and at 1640 cm^{-1} assigned to poly(CB-Ring) and poly(CBOH). Also, the peak area change is noticeable at 1150 cm^{-1} (assigned to C-O stretching), but not as large as for poly(CB-Ring) from pure TFA, further indicating switching is incomplete. When the pH was reduced to 1, the area of the peak at 1640 cm^{-1} reduced significantly, and the area of the peak at 1150 cm^{-1} increased significantly, indicating almost complete switching to poly(CB-Ring). There was little difference between the spectra at pH 0.6 and pH 1. The poly(CBOH) carbonyl peak at 1640 cm^{-1} is barely seen in pH 0.6 and pH 1 spectra indicating almost complete switching. Interestingly, the pK_a value of the sarcosine acid group is 2.1 [38]. It appears that this pK_a value decreases (indicating an increase in acidity of the acid groups) by a full unit as a result of quaternization of the amine group on sarcosine during monomer synthesis [39], perhaps because the quaternary amine is a strong electron-withdrawing group near the carboxylic acid group. Further research is ongoing to increase the switching pH of the polymer chemistry by changing the pK_a of the acid group in the monomer. While using pH 1 cleaning solutions is not unprecedented, it may be desirable to carry out membrane cleaning under less aggressive conditions.

3.4.3 Determination of switching times

Cao et al. [22, 23] report the switching kinetics for the monomer in solution, but not for the

polymer modified gold surfaces used in their study. Poly(CBOH) modified silicon wafers were placed in a TFA/water solution of pH 1 for various times to determine the time required to switch from poly(CBOH) to poly(CB-Ring). Figure 6A shows the FTIR spectra of the poly(CBOH) modified silicon wafers in pH 1 solution for various times. Fifteen minutes (0.25 h) was sufficient to see complete switching, i.e., the peak at 1640 cm^{-1} assigned to carbonyl stretching in poly(CBOH) was absent and the peak area at 1150 cm^{-1} assigned to C-O stretching was greatly increased. A typical cleaning process for membranes lasts 30 min to 1 h [40], so a switching time of 15 min is practical. Poly(CB-Ring) modified silicon wafers were placed in deionized water for various times to determine the time required to switch from poly(CB-Ring) to poly(CBOH). Figure 6B shows the FTIR spectra of the poly(CB-Ring) modified silicon wafers in water for various times. Again, 0.25 h was sufficient to see complete switching, as evidenced by the lack of a peak at 1680 cm^{-1} assigned to carbonyl stretching in poly(CB-Ring) and the decrease in peak area at 1150 cm^{-1} assigned to C-O stretching.

3.4.4 Demonstration of polymer layer stability

To test if the switching mechanism would hold over numerous cycles, the surface of a polymer-modified silicon wafer was switched over 50 cycles. Each cycle comprised placing the poly(CBOH) modified silicon wafer in pure TFA for at least 0.33 h to switch to poly(CB-ring) and then in deionized water for at least 0.33 h to switch back to poly(CBOH). Figure 7 shows the FTIR spectra of the wafers after switching 1, 10, and 50 cycles. Switching was confirmed by the shift in the carbonyl stretching peak from 1640 cm^{-1} to 1680 cm^{-1} and the large increase in peak area from approximately 1150 cm^{-1} to 1200 cm^{-1} (assigned to C-O stretching). The switchability remained after 50 cycles, showing that this chemistry can withstand many cleaning cycles.

3.6. Surface free energy measurements

Surface free energies (SFEs) were calculated for poly(CBOH) modified silicon wafers and poly(CB-Ring) modified silicon wafers by measuring the contact angle of water and diiodomethane on each surface. Table 2 presents the SFE data based on the Owens-Wendt method. Also included are the contact angle data for PEG and three other common zwitterions on silicon wafers for comparison [41, 42]. SFE is a measure of the "stickiness" of a surface, and thus the lower the SFE, the lower the potential for foulants to adsorb to the surface. While the other zwitterions are more hydrophilic than CBOH as indicated by their lower water contact angles, CBOH has a lower affinity (higher contact angle) towards diiodomethane than all but PDMAB. This implies that CBOH could have weaker hydrophobic interactions with biopolymers/microorganisms than the other zwitterions, which would improve its effectiveness as an anti-fouling coating. Both the poly(CBOH) and the poly(CB-Ring) modified silicon wafers had lower SFEs than any of the common anti-fouling coatings. Thus, coating membranes with the poly(CBOH) chemistry was expected to improve biofouling resistance.

3.7. Biofilm studies on membranes

Biofilm studies were performed on unmodified, poly(CBOH) modified, and poly(SPE) modified Microdyn-Nadir PES membranes. Biofilm of a known biofouling bacterium (*Sphingomonas wittichii* RW1) [43] was grown under conditions promoting rapid/strong biofilm growth by providing enrichment of nutrients for biofilm development on unmodified, poly(CBOH) modified, and poly(SPE) modified Microdyn-Nadir PES membranes, and the characteristics of each biofilm were determined. Anti-microbial effects of the grafted layer due to the switching of the poly(CBOH) zwitterion to poly(CB-Ring) quaternary amine were evaluated

by conducting an analysis of the biofilm components (live cells, dead cells and EPS) with CLSM before and after 20 min exposure to 0.1 M HCl (pH 1). Data were compared a control membrane that was modified by grafting a poly(SPE), "non-switchable" zwitterion layer. Figure 8 shows representative biofilm images on unmodified, poly(CBOH) modified, and poly(SPE) modified PES membranes. Table 3 shows the volumetric quantification of the biofilm components (live cells, dead cells, and EPS) for all three membrane types (no acid rinse). The biovolume per membrane area (live and dead cells) was reduced greatly upon surface modification of the PES membranes from 42 $\mu m^3/\mu m^2$ to 19 $\mu m^3/\mu m^2$ (poly(CBOH) modified) and 21 $\mu m^3/\mu m^2$ (poly(SPE) modified) (Figure 8 and Table 3). These results can be seen in Figure 8 where white spots indicate the membrane surface that is devoid of biomass. The corresponding average thickness of biomass was reduced from 70 μm to 36 μm (poly(CBOH) modified) and 39 μm (poly(SPE) modified). Table 4 shows the volumetric quantification of the biofilm components (live cells, dead cells, and EPS) for the poly(CBOH) modified and poly(SPE) modified PES membranes after exposing the biofilms to 0.1 M HCl for 20 min. After acid exposure, the biovolume of dead cells was elevated significantly only for the poly(CBOH) modified membrane (from 4.7 to 9.3 $\mu m^3/\mu m^2$), and the dead to live cells ratio increased from 0.33 to 1.04 (Figure 8 and Tables 3 and 4). A larger number of dead cells and a smaller number of live cells were detected after rinsing with 0.1 M HCl only on the poly(CBOH) modified PES membrane (Figure 8 and Tables 3 and 4). The EPS material was quantified with the fluorescently labeled ConA. EPS biovolume was determined to be statistically different only for the poly(CBOH) modified membrane, and EPS biomass thickness for poly(CBOH) and poly(SPE) modified membranes were determined to be statistically different from the unmodified membrane. The reductions in dead and live biovolume and biomass thickness on the poly(CBOH) and poly(SPE) modified

membranes (before exposure to 0.1 M HCl) relative to unmodified membrane were found to be statistically different at the 95% confidence level (Table S1). Also the elevation of dead cell biovolume and thickness and the reduction of live cell biomass thickness on the poly(CBOH) modified membranes before and after exposure to 0.1 M HCl were found to be statistically different at the 95% confidence level based on a two-tailed t-test (Table S2). The reduction in biomass on the poly(CBOH) and on the poly(SPE) modified PES membranes can be attributed to the increase in hydrophilicity and hydration of the grafted zwitterion layers (Figure S7). The dead and live cell biovolume and the live cell biomass thickness on the poly(SPE) modified membranes before and after exposure to 0.1 M HCl were found to be statistically the same at 95% confidence (Table S3). While the overall number of cells and EPS on the poly(CBOH) modified and poly(SPE) modified PES membranes did not changed after exposure to 0.1 M HCl (Tables 3 and 4), biofilm mortality was higher on the poly(CBOH) coated membrane. This mortality, expressed as the dead to live cells ratio, was likely enhanced by the anti-microbial, quaternary amine group of the poly(CB-ring) layer (Figure 1) upon exposure to the pH 1.0 acid solution, since no enhancement was found for the non-switchable poly(SPE) coated membrane.

Interestingly, the total biomass roughness was much higher for poly(CBOH) modified and poly(SPE) modified PES membranes (both before and after exposure to 0.1 M HCl) than for unmodified PES membranes. A possible reason is because there is a more fully developed biofilm on the unmodified membranes, which would present a smoother surface than a patchy, less well developed biofilm on the poly(CBOH) modified and poly(SPE) modified membranes (as it appears in Figure 8) [44]. This patchiness of the biofilm on the poly(CBOH) modified and poly(SPE) modified membranes shows a slower rate of biofilm development on the modified membranes, further indicating the modification layers effectiveness towards biofouling control.

4. Conclusions

A method was developed for applying a new type of zwitterionic surface chemistry onto polyethersulfone ultrafiltration membranes to reduce membrane biofouling. Poly(CBOH) modified PES membranes reduced the bacteria deposition coefficient by an order of magnitude from unmodified PES, and less than half the amount of biofilm biomass was developed onto the modified membrane surface compared to the unmodified membrane. The enhanced fouling resistance of the poly(CBOH) modified PES membranes is attributed to the increase in surface hydrophilicity and hydration of the grafted polymer layer. A unique feature of this chemistry is its ability to switch from zwitterionic to cationic states. The short time required to switch from a low fouling zwitterion surface to an antimicrobial quaternary amine surface is practical for use. Biofilm mortality was elevated once the anti-fouling poly(CBOH) zwitterion was switched to the anti-microbial, poly(CB-Ring) quaternary amine. Ongoing work is exploring ways to increase the switching pH such that membrane cleaning can be done under less aggressive conditions.

Appendix A. Supplementary material

Supplementary data associated with this article can be found in the online version.

Acknowledgements

SW was supported by a National Science Foundation Graduate Research Fellowship under Award DGE-1246875. Any opinion, findings, and conclusions or recommendations expressed in this material are those of the authors and do not necessarily reflect the views of the NSF. We thank the US-Israel Binational Agricultural Research and Development Fund for financial

support under Research Grant Agreement No. US-4654-13. We thank Alex Kitaygorodskiy in the Clemson University Chemistry Department for assistance with NMR measurements.

Abbreviations

a.u. – absorbance units

AIBN – azobisisobutyronitrile

AFM – atomic force microscopy

ATR-FTIR - attenuated total reflectance Fourier-transform infrared spectroscopy

ATRP – atom transfer radical polymerization

BP - benzophenone

BPA - 2-bromo-2-methylpropionic acid

BPY - 2,2'-bipyridyl

CBOH – 2-((2-hydroxy-3-(methacryloyloxy)propyl)dimethylammonio)acetate

CB-Ring – 2-(methacryloyloxymethyl)-4,4-dimethyl-6-oxomorpholin-4-ium

CBtBu – N-(2-tert-butoxy-2-oxoethyl)-2-hydroxy-3-(methacryloyloxy)-N,N-dimethylpropan-1-aminium iodide

CLSM – confocal laser scanning microscopy

DCM - dichloromethane

DMF - N,N-dimethylformamide

FTIR - Fourier-transform infrared spectroscopy

GFP – green fluorescent protein

GMA – glycidyl methacrylate

GPC – gel permeation chromatography

LB – Luria-Bertani

MBAA - N,N’-methylenebis(acrylamide)

PDMAB – poly(4-[dimethyl(2’-methacryloyloxyethyl)ammonio]butanoate)

PEG – poly(ethylene glycol)

PEGMA - poly(ethylene glycol) methacrylate

PES – polyethersulfone

PMAPS – poly(3-[dimethyl(2’-methacryloyloxyethyl)ammonio]propanesulfonate)

PMPC – poly(2-(methacryloyloxy)ethyl phophorylcholine)

SFE – surface free energy

SPE - [2-(methacryloyloxy)ethyl]dimethyl-(3-sulfopropyl)ammonium hydroxide

THF – tetrahydrofuran

TFA – trifluoroacetic acid

References

[1] W. Guo, H.-H. Ngo, J. Li, Bioresource technology 2012, 122, 27.
[2] T. Nguyen, F. A. Roddick, L. Fan, Membranes 2012, 2, 804; H.-C. Flemming, G. Schaule, T. Griebe, J. Schmitt, A. Tamachkiarowa, Desalination 1997, 113, 215.
[3] O. Habimana, A. Semião, E. Casey, Journal of Membrane Science 2014, 454, 82.
[4] M. Herzberg, M. Elimelech, Journal of Membrane Science 2007, 295, 11.
[5] G.-d. Kang, Y.-m. Cao, Water research 2012, 46, 584; D. Rana, T. Matsuura, Chemical reviews 2010, 110, 2448; V. Kochkodan, N. Hilal, Desalination 2015, 356, 187; V. Kochkodan, D. J. Johnson, N. Hilal, Advances in colloid and interface science 2014, 206, 116.
[6] E. Ostuni, R. G. Chapman, R. E. Holmlin, S. Takayama, G. M. Whitesides, Langmuir 2001, 17, 5605; Q. Wei, T. Becherer, S. Angioletti-Uberti, J. Dzubiella, C. Wischke, A. T. Neffe, A. Lendlein, M. Ballauff, R. Haag, Angewandte Chemie International Edition 2014, 53, 8004.
[7] G.-d. Kang, Z.-n. Liu, H.-j. Yu, Y.-m. Cao, Desalination and Water Treatment 2012, 37, 139.
[8] B. T. McVerry, M. C. Wong, K. L. Marsh, J. A. Temple, C. Marambio-Jones, E. Hoek, R. B. Kaner, Macromolecular rapid communications 2014, 35, 1528.
[9] Y.-C. Chiang, Y. Chang, C.-J. Chuang, R.-C. Ruaan, Journal of Membrane Science 2012, 389, 76; S. Tada, C. Inaba, K. Mizukami, S. Fujishita, M. Gemmei-Ide, H. Kitano, A. Mochizuki, M. Tanaka, T. Matsunaga, Macromolecular bioscience 2009, 9, 63.
[10] Y. Zhang, Z. Wang, W. Lin, H. Sun, L. Wu, S. Chen, Journal of Membrane Science 2013, 446, 164.
[11] M. L. M. Tirado, M. Bass, M. Piatkovsky, M. Ulbricht, M. Herzberg, V. Freger, Journal of Membrane Science 2016, 520, 490.
[12] F. Razi, I. Sawada, Y. Ohmukai, T. Maruyama, H. Matsuyama, Journal of Membrane Science 2012, 401, 292; P.-S. Liu, Q. Chen, S.-S. Wu, J. Shen, S.-C. Lin, Journal of Membrane Science 2010, 350, 387.
[13] M. Hadidi, A. L. Zydney, Journal of Membrane Science 2014, 452, 97.
[14] S. T. Weinman, S. M. Husson, Journal of Membrane Science 2016, 513, 146.
[15] J. C. Tiller, C.-J. Liao, K. Lewis, A. M. Klibanov, Proceedings of the National Academy of Sciences 2001, 98, 5981; Y.-F. Yang, H.-Q. Hu, Y. Li, L.-S. Wan, Z.-K. Xu, Journal of Membrane Science 2011, 376, 132.
[16] A. Tiraferri, C. D. Vecitis, M. Elimelech, ACS applied materials & interfaces 2011, 3, 2869; F. o. Perreault, M. E. Tousley, M. Elimelech, Environmental Science & Technology Letters 2013, 1, 71.
[17] W.-R. Li, X.-B. Xie, Q.-S. Shi, H.-Y. Zeng, O.-Y. You-Sheng, Y.-B. Chen, Applied microbiology and biotechnology 2010, 85, 1115; J. Yin, Y. Yang, Z. Hu, B. Deng, Journal of Membrane Science 2013, 441, 73.
[18] L. Mi, S. Jiang, Angewandte Chemie International Edition 2014, 53, 1746.
[19] M. S. Rahaman, H. Thérien-Aubin, M. Ben-Sasson, C. K. Ober, M. Nielsen, M. Elimelech, Journal of Materials Chemistry B 2014, 2, 1724; I. Sawada, R. Fachrul, T. Ito, Y. Ohmukai, T. Maruyama, H. Matsuyama, Journal of Membrane Science 2012, 387, 1; G. M. Nisola, J. S. Park, A. B. Beltran, W.-J. Chung, RSC Advances 2012, 2, 2439.
[20] P. Zou, W. Hartleb, K. Lienkamp, Journal of Materials Chemistry 2012, 22, 19579; G. Ye, J. Lee, F. Perreault, M. Elimelech, ACS applied materials & interfaces 2015, 7, 23069; Y. Sui, X. Gao, Z. Wang, C. Gao, Journal of membrane science 2012, 394, 107; Y. Mei, C. Yao, X. Li, Biofouling 2014, 30, 313; J. Jiang, L. Zhu, L. Zhu, H. Zhang, B. Zhu, Y. Xu, ACS applied materials & interfaces 2013, 5, 12895.
[21] Q. Yu, J. Cho, P. Shivapooja, L. K. Ista, G. P. López, ACS Applied Materials & Interfaces 2013, 5, 9295.
[22] Z. Cao, N. Brault, H. Xue, A. Keefe, S. Jiang, Angewandte Chemie International Edition 2011, 50, 6102.

[23] Z. Cao, L. Mi, J. Mendiola, J. R. Ella-Menye, L. Zhang, H. Xue, S. Jiang, Angewandte Chemie International Edition 2012, 51, 2602.
[24] B. Cao, L. Li, Q. Tang, G. Cheng, Biomaterials 2013, 34, 7592; B. Cao, Q. Tang, L. Li, J. Humble, H. Wu, L. Liu, G. Cheng, Advanced healthcare materials 2013, 2, 1096.
[25] H. C. Chenette, J. M. Welsh, S. M. Husson, Separation Science and Technology 2017, 52, 276.
[26] B. V. Bhut, S. R. Wickramasinghe, S. M. Husson, Journal of Membrane Science 2008, 325, 176.
[27] D. K. Owens, R. Wendt, Journal of applied polymer science 1969, 13, 1741; A. Rudawska, E. Jacniacka, International Journal of Adhesion and Adhesives 2009, 29, 451.
[28] K. Baransi-Karkaby, M. Bass, S. Levchenko, S. Eitan, V. Freger, Environmental Science & Technology 2017, 51, 2347.
[29] W. Ying, R. Kumar, M. Herzberg, R. Kasher, Environmental science & technology 2015, 49, 6815; W. Ying, N. Siebdrath, W. Uhl, V. Gitis, M. Herzberg, Journal of Membrane Science 2014, 466, 26.
[30] R. Bernstein, V. Freger, J.-H. Lee, Y.-G. Kim, J. Lee, M. Herzberg, Biofouling 2014, 30, 367.
[31] R. Murga, P. S. Stewart, D. Daly, Biotechnology and bioengineering 1995, 45, 503.
[32] A. Heydorn, A. T. Nielsen, M. Hentzer, C. Sternberg, M. Givskov, B. K. Ersbøll, S. Molin, Microbiology 2000, 146, 2395.
[33] M. Bass, V. Freger, Journal of Membrane Science 2015, 492, 348.
[34] D. He, H. Susanto, M. Ulbricht, Progress in Polymer Science 2009, 34, 62.
[35] M. Ulbricht, H. Yang, Chemistry of materials 2005, 17, 2622.
[36] M. Birkner, M. Ulbricht, Journal of Membrane Science 2015, 494, 57; P. Kaner, D. J. Johnson, E. Seker, N. Hilal, S. A. Altinkaya, Journal of Membrane Science 2015, 493, 807.
[37] R. M. Silverstein, F. X. Webster, D. J. Kiemle, *Spectrometric Identification of Organic Compounds*, John Wiley & Sons, Inc., 2011.
[38] R. M. C. Dawson, D. C. Elliot, W. H. Elliot, K. M. Jones, *Data for biochemical research*, Oxford University Press, 1986.
[39] D. B. Thomas, Y. A. Vasilieva, R. S. Armentrout, C. L. McCormick, Macromolecules 2003, 36, 9710.
[40] W. S. Ang, S. Lee, M. Elimelech, Journal of Membrane Science 2006, 272, 198; A. Subramani, E. M. Hoek, Desalination 2010, 257, 73.
[41] O. Moreau, C. Portella, F. Massicot, J. Herry, A. Riquet, Surface and Coatings Technology 2007, 201, 5994.
[42] M. Kobayashi, Y. Terayama, H. Yamaguchi, M. Terada, D. Murakami, K. Ishihara, A. Takahara, Langmuir 2012, 28, 7212.
[43] L. Bereschenko, A. Stams, G. Euverink, M. Van Loosdrecht, Applied and environmental microbiology 2010, 76, 2623.
[44] D. Janjaroen, F. Ling, G. Monroy, N. Derlon, E. Mogenroth, S. A. Boppart, W.-T. Liu, T. H. Nguyen, Water research 2013, 47, 2531.

Tables

Table 1. *Pseudomonas fluorescens* deposition (mass transfer) coefficients of unmodified GE Osmonics PES membranes and membranes modified with poly(CBOH), poly(SPE), and poly(PEGMA) by UV polymerization. Uncertainties represent one standard deviation among at least four different membrane samples.

Sample	k_d (μm/min)
Unmodified PES	1.4 ± 0.33
poly(CBOH) modified	0.10 ± 0.07
poly(SPE) modified	0.13 ± 0.07
poly(PEGMA) modified	0.18 ± 0.07

Table 2. Water and diiodomethane contact angles for silicon wafers modified with poly(CBOH) and poly(CB-Ring). Contact angle data are included for common antifouling chemistries: PEG, PMAPS (sulfobetaine zwitterion), PDMAB (carboxybetaine zwitterion), and PMPC (phosphobetaine zwitterion) on silicon wafers. Surface energy calculations are based on the Owens-Wendt method. Uncertainties represent the data range from at least 3 measurements or the error values reported in the articles cited.

	Contact Angle (degree)		Surface energies (mJ/m^2)		
	Water	**CH_2I_2**	**Dispersive**	**Polar**	**Total**
poly(CBOH)	41 ± 1	40 ± 1	30 ± 1	29 ± 1	59 ± 1
poly(CB-Ring)	42 ± 4	50 ± 1	25 ± 0	31 ± 3	57 ± 2
PEG [41]	39 ± 1	14 ± 3	40 ± 1	24 ± 1	64 ± 1
PMAPS [42]	11 ± 2	30 ± 2	32 ± 1	41 ± 1	73 ± 1
PDMAB [42]	16 ± 1.5	40 ± 2	28 ± 1	42 ± 2	71 ± 1
PMPC [42]	< 3	27 ± 2	34 ± 1	41 ± 1	75 ± 1

Table 3. Biofilm volumetric quantification (biomass volume per membrane area, biomass thickness, and bio coefficient) for each component of the biofilm formatted by *Sphingomonas wittichii* RW1 on unmodified, po poly(SPE) modified Microdyn-Nadir PM UP150 PES membranes. Uncertainties represent one standard devia data points.

Membrane	**Unmodified PES**			**poly(CBOH)-PES**			
	dead	**live**	**EPS**	**dead**	**live**	**EPS**	**dead**
Biomass ($\mu m^3/\mu m^2$ membrane)	16.7 ± 2.5	25.2 ± 1.7	4.0 ± 0.8	4.7 ± 1.3	14.0 ± 2.6	2.2 ± 1.2	6.8 ± 1.6
Biomass Thickness (μm)	33.5 ± 4.4	36.5 ± 4.4	13.7 ± 2.6	9.6 ± 3.6	26.5 ± 5.1	3.1 ± 1.4	12.5 ± 2.8
Biomass Roughness Coefficient	0.1 ± 0.03	0.07 ± 0.02	1.2 ± 0.08	1.4 ± 0.7	0.1 ± 0.1	1.8 ± 1.5	1.0 ± 0.4

Table 4. Biofilm volumetric quantification (biomass volume per membrane area, biomass thickness, and bio
coefficient) for each component of the biofilm formatted by *Sphingomonas wittichii* RW1 on poly(CBOH) m
modified Microdyn-Nadir PM UP150 PES membranes after pH 1.0 acid treatment for 20 min. Uncertainties
deviation amongst at least eight data points.

Membrane after Acid treatment (pH 1)	**poly(CBOH)-PES**			**poly(SPE)-PES**		
	dead	**live**	**EPS**	**dead**	**live**	**EPS**
Biomass ($\mu m^3/\mu m^2$ membrane)	9.4 ± 2.5	8.9 ± 7.8	1.9 ± 1.8	8.2 ± 2.5	13.9 ± 3.4	1.0 ± 0.9
Biomass Thickness (µm)	17.7 ± 4.4	14.7 ± 10.4	3.0 ± 2.9	17.0 ± 4.3	25.9 ± 6.1	0.2 ± 0.1
Biomass Roughness Coefficient	0.7 ± 0.4	0.8 ± 1.0	1.9 ± 0.7	0.8 ± 0.5	0.1 ± 0.09	2.0 ± 0.01

Figures

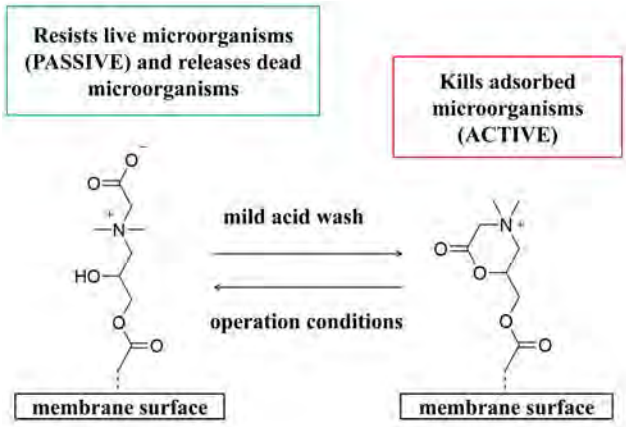

Figure 1. Switching schematic between the anti-fouling, zwitterion chemistry (CBOH, left) and the anti-microbial, quaternary amine chemistry (CB-Ring, right). CBOH would switch to CB-Ring when exposed to a typical cleaning solution for membranes, and CB-Ring would switch to CBOH when exposed back to normal operating conditions.

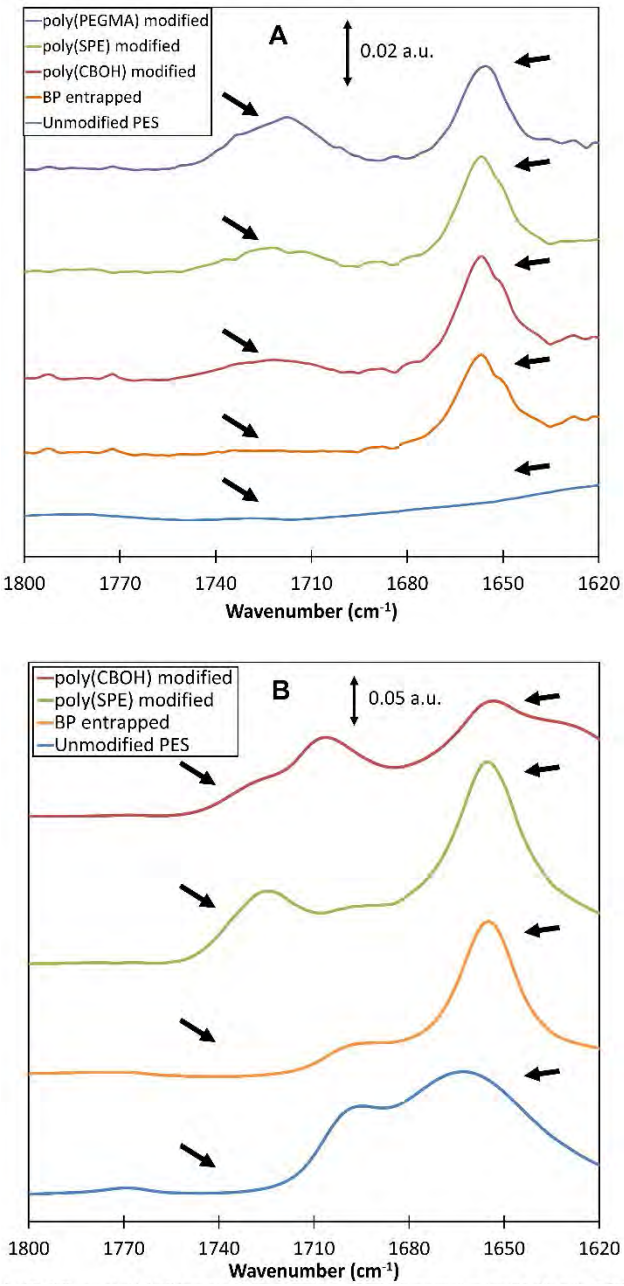

Figure 2. ATR-FTIR spectra of (A) GE Osmonics PW membranes unmodified, BP entrapped, and modified by poly(CBOH), poly(SPE), and poly(PEGMA) and (B) Microdyn-Nadir PM UP150 PES membranes unmodified, BP entrapped, and modified by poly(SPE) and poly(CBOH). Scale bar represents (A) 0.02 absorbance units (a.u.) and (B) 0.05 absorbance units (a.u.). Color version of figure can be found online.

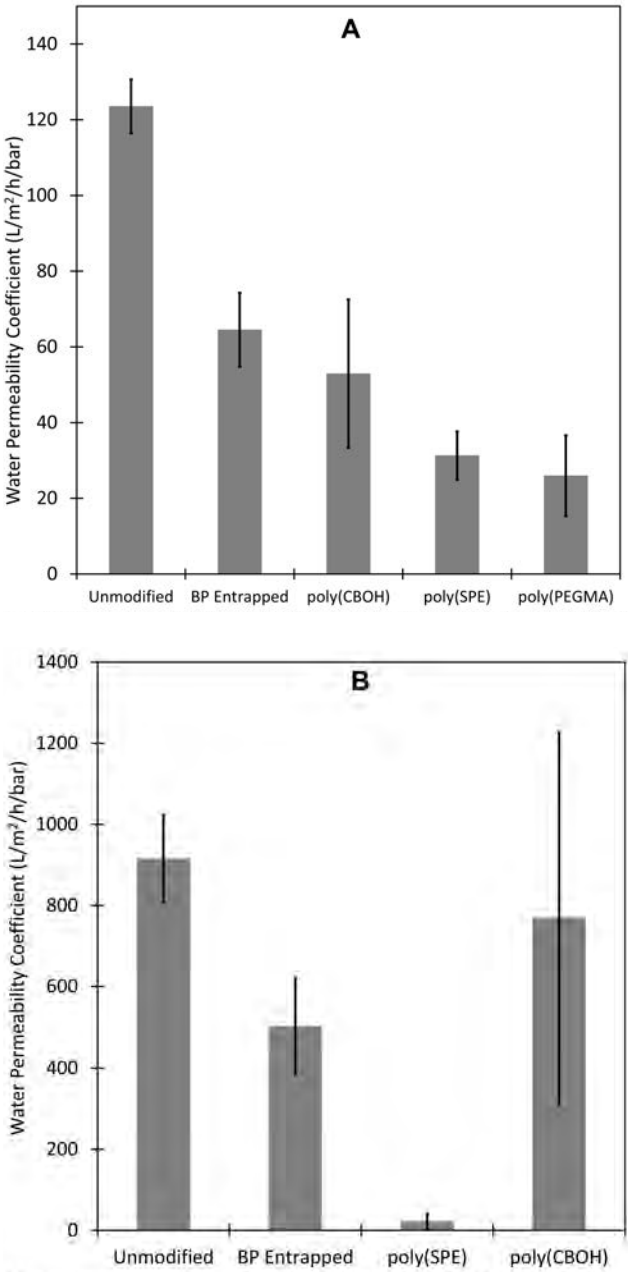

Figure 3. Pure water permeability coefficient (L/m^2/h/bar) versus modified membrane type for (A) unmodified, BP entrapped, and modified by poly(CBOH), poly(SPE), and poly(PEGMA) GE PW and (B) unmodified, BP entrapped, poly(SPE) modified, and poly(CBOH) modified Microdyn-Nadir PM UP150 PES membranes. Membranes were tested in dead-end configuration and the testable membrane area was 14.6 cm^2. Error bars represent one standard deviation among at least 4 samples.

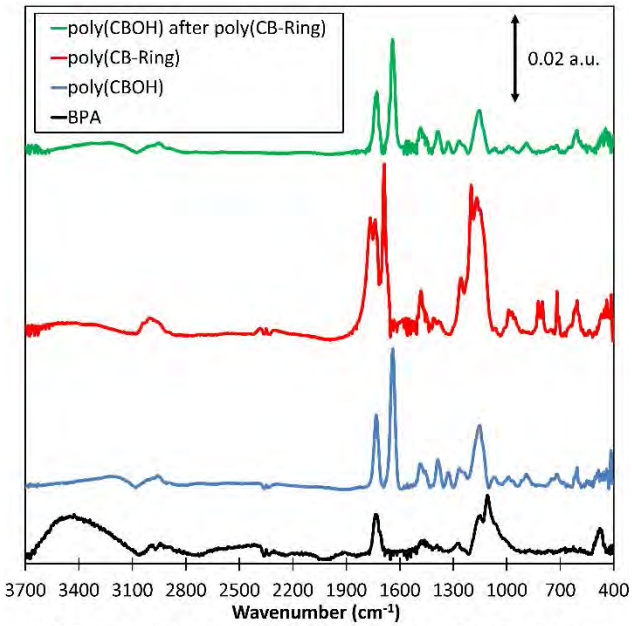

Figure 4. FTIR spectra of silicon wafers surface modified with initiator (BPA), poly(CBOH), poly(CB-Ring) (poly(CBOH) after immersion in TFA for 1 h), and poly(CBOH) after poly(CB-Ring) (poly(CB-Ring) after immersion in deionized water for 1 h). Poly(CBOH) layer thickness was approximately 60 nm. Scale bar represents 0.02 absorbance units (a.u.). Color version of figure can be found online.

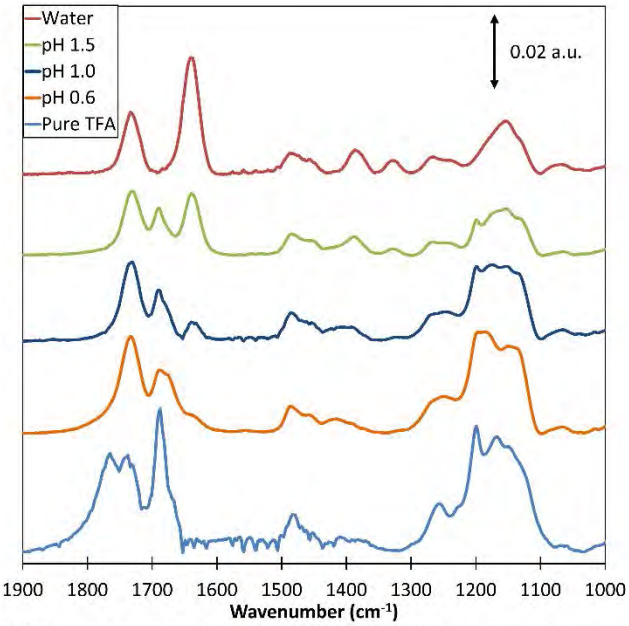

Figure 5. FTIR spectra of poly(CBOH) modified silicon wafers after being immersed in deionized water, TFA, and TFA/water solutions at pH values of 0.6, 1.0, and 1.5 for 1 h. The evolution of the peak at 1680 cm^{-1} and the increase in peak area at 1150 cm^{-1} indicates conversion from poly(CBOH) to poly(CB-Ring). Poly(CBOH) layer thickness is approximately 60 nm. Scale bar represents 0.02 absorbance units. Color version of figure can be found online.

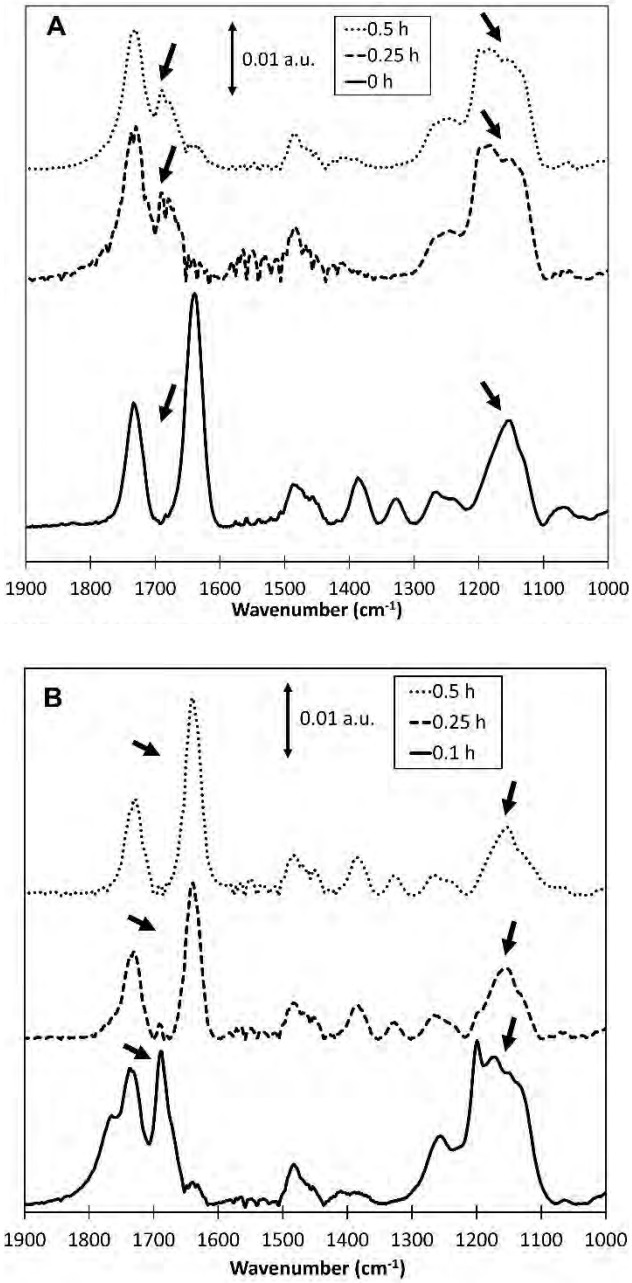

Figure 6. FTIR spectra of (A) poly(CBOH) modified silicon wafers conversion to poly(CB-Ring) by immersion in a TFA/water solution of pH 1.0 for 0 h, 0.25 h, and 0.5 h and (B) poly(CB-Ring) modified silicon wafers conversion to poly(CBOH) by immersion in deionized water for 0.1 h, 0.25 h, and 0.5 h. Poly(CBOH) layer thickness is approximately 60 nm. The scale bar in each figure represents 0.01 absorbance units.

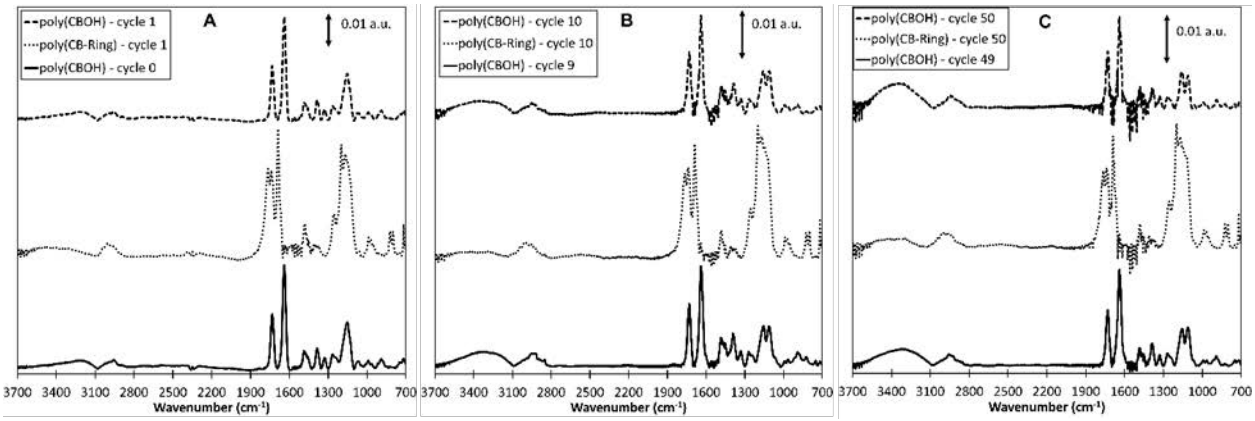

Figure 7. FTIR spectra of silicon wafers surface modified with poly(CBOH), poly(CB-Ring) (prepared by immersion of the poly(CBOH) sample in TFA for 0.33 h), and poly(CBOH) (prepared by immersion of the poly(CB-Ring) sample in deionized water for 0.33 h). The number of cycles of switching from poly(CBOH) to poly(CB-Ring) back to poly(CBOH) are shown in the legends of (A) 0-1, (B) 9-10, and (C) 49-50. Poly(CBOH) layer thickness is approximately 60 nm. Scale bar represents 0.01 absorbance units (a.u.).

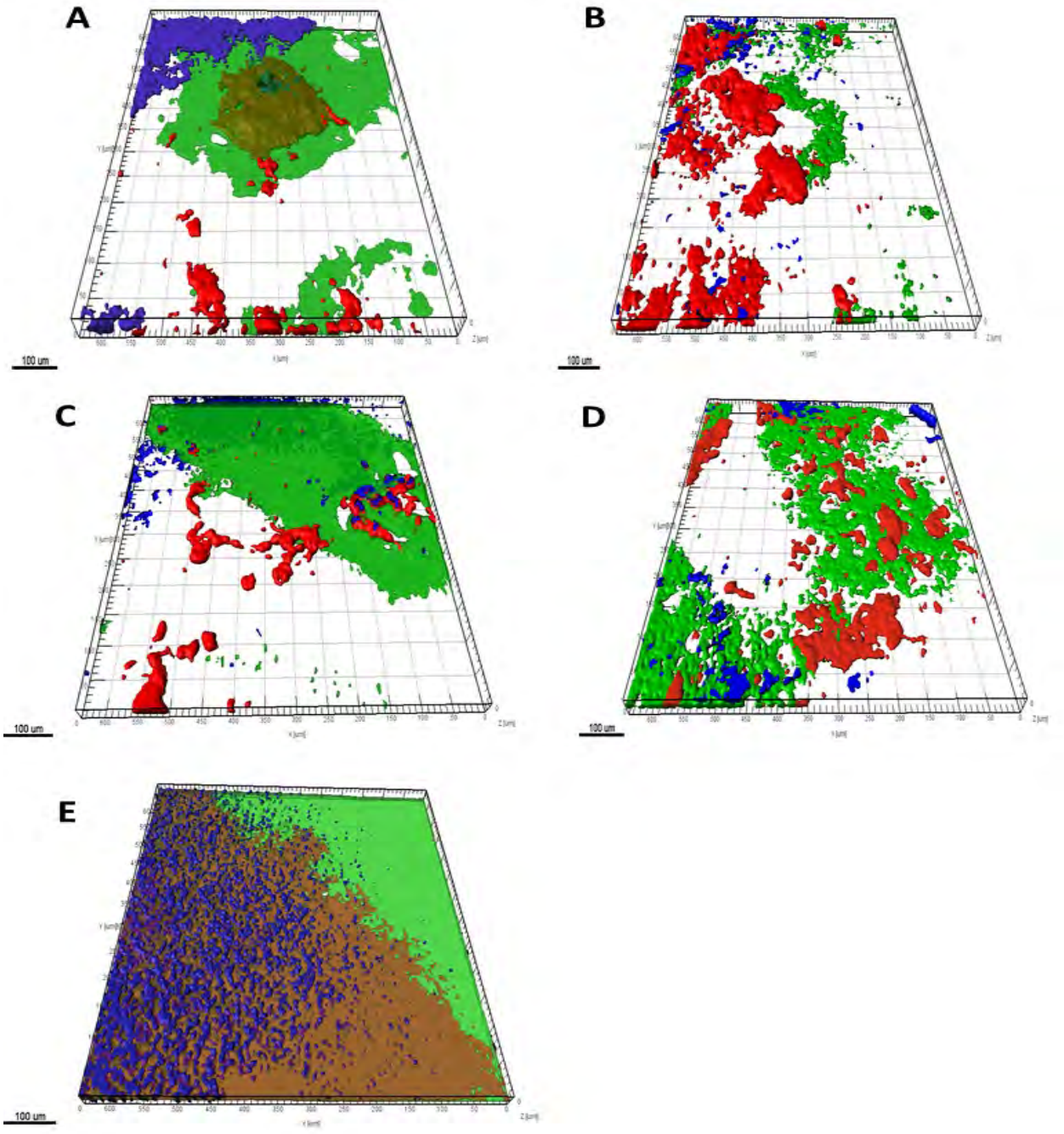

Figure 8. CLSM images of the biofilm development by *Sphingomonas wittichii* RW1 on poly(CBOH) modified (top, A-B), poly(SPE) modified (middle, C-D) and pristine (bottom, E) Microdyn-Nadir PM UP150 PES membrane. Red, blue and green represent non-viable bacteria, EPS and viable bacteria. Figure 4A, 4C, and 4E represents biofilm on poly(CBOH) modified, poly(SPE) modified, and unmodified PES membrane respectively; while 4B and 4D indicates

biofilm formation on the acid treated poly(CBOH) modified and poly(SPE) modified PES membrane, respectively. The deep orange color indicates overlapping zone of dead and live cells. Images are 635 μm × 635 μm and the scale bar represents 100 μm. Color version of figure can be found online.

Graphical Abstract

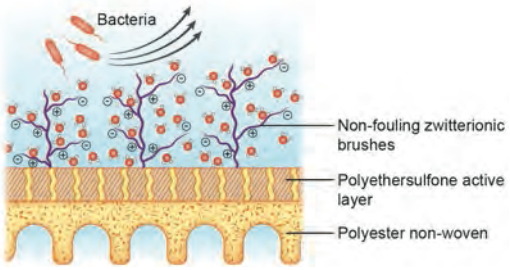

A switchable zwitterionic membrane surface chemistry for biofouling control

Steven T. Weinman,[†] Maria Bass,[§] Soumya Pandit, [‡] Moshe Herzberg,[‡] Viatcheslav Freger,[§] Scott M. Husson[*,†]

[†]Department of Chemical and Biomolecular Engineering, Clemson University, Clemson, SC 29634, USA

[§]Wolfson Department of Chemical Engineering, Technion - Israel Institute of Technology, Haifa, 32000 Israel

[‡]Zuckerberg Institute for Water Research, Ben Gurion University of the Negev, Sede-Boqer Campus, Midreshet Ben Gurion, 84990 Israel

*Corresponding author: Tel: +1 (864)-656-4502, Fax: +1 (864)-656-0784. Email address: shusson@clemson.edu

Supporting Information

Surface Modification via ATRP

Silicon wafer substrates were cleaned prior to PGMA deposition. Substrates were cleaned in deionized water in test tubes by placing them in an ultrasonic bath for 20 min. The substrates were dried and put in new test tubes. Cleaned substrates were placed in a 1:3 (v/v) mixture of hydrogen peroxide and sulfuric acid at 80-90 °C for 1 h. [*Caution Piranha solution*: this mixture reacts violently with organic compounds. It should be used in small volumes with proper supervision and safety wear. Special precautions should be exercised in its disposal to avoid contact with organics.] Next, the substrates were rinsed thoroughly with de-ionized water and dried. PGMA deposition and BPA initiation details were presented in the manuscript.

Figure S1 depicts the ATRP process for poly(CBOH). Poly(CBOH) was grown from initiator-functionalized silicon wafer substrates by surface-initiated ATRP similar to Cao et al. [1], but with minor modifications. Activator, copper (I) bromide (0.1 M), and amine ligand, BPY (0.3 M), were put in 3:1 (v/v) mixture of DMF and deionized water inside the glovebox. The mixture was sealed inside the glovebox and was placed in an ultrasonic bath for 2 h outside the glovebox to form the activator/ligand complex. CBOH monomer (0.1 M) was added to the solution inside the glovebox and was mixed until dissolved. Polymerization was carried out by placing an initiator-functionalized substrate into this reaction mixture. Polymerization was done at 35 °C for 3 h. Polymerization was terminated by removing the substrates from the reaction mixture and washing thoroughly with a 3:1 (v/v) DMF and deionized water mixture.

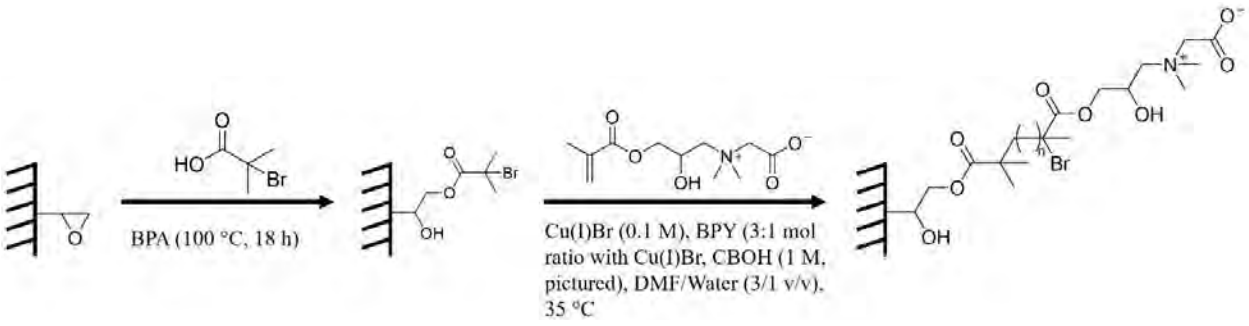

Figure S1. ATRP reaction schematic. BPA initiator is reacted with epoxide of PGMA and CBOH is polymerized from radical initiator by ATRP.

Surface Modification via UV Polymerization

UV polymerization was performed to graft poly(CBOH), poly(PEGMA), and poly(SPE) from PES ultrafiltration membranes. Figure S2 depicts the BP entrapment process and the UV polymerization process for poly(CBOH). Experiment details are given in the manuscript (Section 2.2.1.).

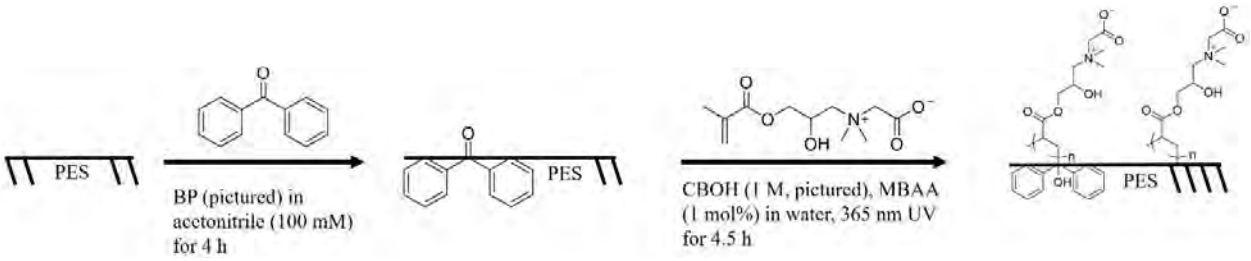

Figure S2. UV-photopolymerization schematic. BP is entrapped within PES to increase the reaction site density. CBOH is polymerized from both BP radicals and PES radicals.

Ellipsometry

Multi-angle ellipsometry (Beaglehole Instruments, Picometer) was used to measure the dry thicknesses of PGMA, BPA, and poly(CBOH) layers on silicon wafers. The incident beam was produced by a 632.8 nm He–Ne laser source. Measurements were done at incidence angles from 56° to 80° with a step size of 4°. The reported thickness is the average of five random locations on each wafer. In this study, an air–poly(CBOH)–BPA–PGMA–silicon dioxide–silicon substrate multilayer model was applied to fit the data based on a Cauchy model. Layer thickness was allowed to vary and refractive index was fixed (air = 1.0, poly(CBOH) = 1.5, BPA = 1.451, PGMA = 1.525, silicon dioxide = 1.455, and silicon = 3.875). Layer thickness was calculated by IgorPro Software version 4.09A. Silicon dioxide thickness was 1.8 nm, PGMA thickness was 8-12 nm, BPA thickness was 3-5 nm, and poly(CBOH) thickness was 45-70 nm.

Surface Energy Calculations

Equation S1 was used to calculate the surface free energy (SFE) of silicon wafers:

$$\gamma_s = \gamma_s^d + \gamma_s^p \quad \text{(S1)}$$

γ_s is the SFE of the silicon wafer, γ_s^d is the dispersion component of the SFE of the silicon wafer, and γ_s^p is the polar component of the SFE of the silicon wafer. Two liquids with different surface free energy components were used to determine the dispersion and polar components of the SFE. Using the SFE values (total, polar, and dispersion) for each fluid and the respective contact angles of each fluid on the silicon wafers, Equations S2 and S3 were used to calculate the dispersion and polar components of the silicon wafer SFE [2].

$$\sqrt{\gamma_s^d} = \frac{\gamma_d(\cos\theta_d+1)-\gamma_w(\cos\theta_w+1)\sqrt{(\gamma_d^p/\gamma_w^p)}}{2\left(\sqrt{\gamma_d^d}-\sqrt{\gamma_d^p(\gamma_w^d/\gamma_w^p)}\right)} \quad \text{(S2)}$$

$$\sqrt{\gamma_s^p} = \frac{\gamma_w(\cos\theta_w+1)-2\sqrt{\gamma_s^d\gamma_w^d}}{2\sqrt{\gamma_w^p}} \quad \text{(S3)}$$

γ_d is the SFE of diiodomethane (50.8 mJ/m^2) [3], γ_d^d is the dispersive component of the diiodomethane SFE (49.5 mJ/m^2) [3], γ_d^p is the polar component of the diiodomethane SFE (1.3 mJ/m^2) [3], γ_w is the SFE of water (72.8 mJ/m^2) [3], γ_w^d is the dispersive component of the water SFE (21.8 mJ/m^2) [3], γ_w^p is the polar component of the water SFE (51 mJ/m^2) [3], θ_d is the diiodomethane contact angle, and θ_w is the water contact angle. Data for SFE are presented in Table 3 in the manuscript.

NMR

^{1}H-NMR was performed with a 300 MHz NMR spectrometer (Bruker Avance) equipped with a 5 mm quadruple nucleus probe. The spectra were acquired from -4.1 to 16.5 ppm with a 30° pulse, an acquisition time of 2.65 s, and a total of 16 scans were collected per sample. Samples were dissolved at a concentration of 50 mg/mL in chloroform-d (CBtBu), deuterium

oxide (CBOH), or trifluoroacetic acid-d (CB-Ring) with tetramethylsilane as a reference peak. Integration and peak identification were performed with TopSpin 2.1 software (Bruker Corp.).

^{13}C-NMR was performed using the same 300 MHz NMR spectrometer. The spectra were acquired from -20 to 220 ppm and a total of at least 512 scans were collected per sample. Samples were dissolved at a concentration of 50 mg/mL in chloroform-d (CBtBu), deuterium oxide (CBOH), or trifluoroacetic acid-d (CB-Ring) with tetramethylsilane as a reference peak. Peak identification was performed with TopSpin 2.1 software (Bruker Corp.).

CBtBu Synthesis

Figure S3 shows the process for the entire CBOH monomer synthesis. Sarcosine *tert*-butyl ester hydrochloride was dissolved in water (6.5 mL water/g sarcosine *tert*-butyl ester hydrochloride) and neutralized with sodium bicarbonate (1.5 mol sodium bicarbonate:1 mol sarcosine *tert*-butyl ester hydrochloride) for 1 h under stirring. Sarcosine *tert*-butyl ester was extracted with chloroform (1:1 v/v, 2 times) and then reacted with uninhibited GMA (1.5 mol GMA:1 mol sarcosine *tert*-butyl ester hydrochloride) in chloroform using zinc tetrafluoroborate hydrate (1 mol zinc tetrafluoroborate hydrate:10 mol sarcosine *tert*-butyl ester hydrochloride) as a catalyst. This reaction was done in a microwave reactor (MARS5, CEM) at 140 °C for 2 h. Undissolved catalyst and byproduct PGMA generated during the reaction was removed by filtration (Whatman™ hardened low ash grade 50 filter paper, GE Healthcare Life Sciences). Iodomethane (20 mol iodomethane:1 mol sarcosine *tert*-butyl ester hydrochloride) was reacted with the monomer solution for 6 h under stirring to quaternize the nitrogen. The protected monomer (CBtBu) was precipitated in diethyl ether, filtered out (same filter paper as above), and dried under vacuum at 20-25 °C and -0.78 to -0.95 barg. Figure S4 depicts a typical ^{1}H-NMR

and ^{13}C-NMR of CBtBu. Yield was approximately 85 mol% with approximately 85% purity as determined by NMR. Cao et al. [1] provided an interpretation for each NMR spectrum, however an interpretation is provided based on the results obtained from the experiments described. The following is the interpretation of the ^{1}H-NMR spectrum in Figure S4A, with lowercase letters assigned to identify each proton type as assigned in the image: 1.49 (a), 1.94 (i), 3.55-3.66 (c), 3.74-4.07 (d), 4.22-4.24 (b), 4.48-4.70 (f), 4.74-4.78 (e), 5.62-5.63 (h), 6.18 (g), 7.28 (residual chloroform). The following is the interpretation of the ^{13}C-NMR spectrum in Figure S4B, with lowercase letters assigned to identify each carbon type as assigned in the image: 18.30 (l), 27.94 (a), 53.8-54.5 (e), 62.57 (d), 63.51 (g), 65.19 (f), 65.81 (h),76.5-77.5 (residual chloroform), 85.41 (b), 126.90 (j), 135.37 (k), 163.34 (i), 166.99 (c).

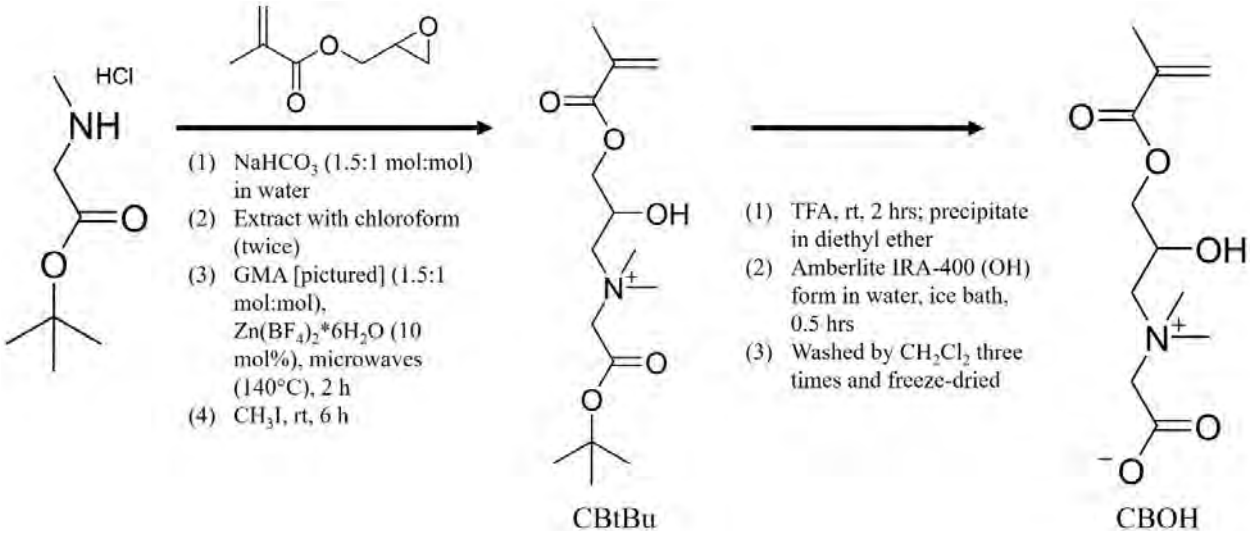

Figure S3. Monomer synthesis schematic. CBtBu is the protected monomer and CBOH is the zwitterion monomer used in experiments.

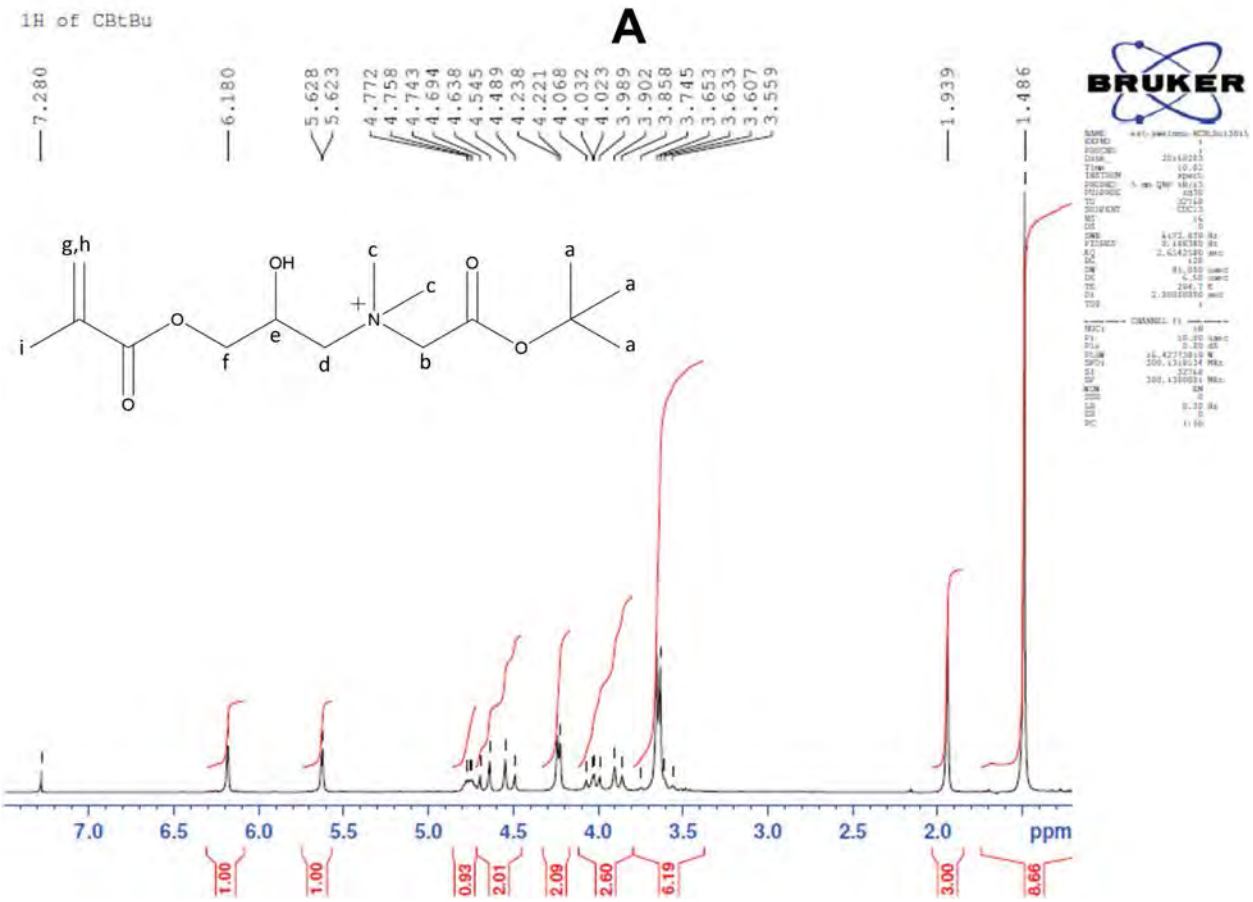
1H of CBtBu
A
7.280
6.180
5.628
5.623
4.772
4.758
4.743
4.694
4.638
4.545
4.489
4.238
4.221
4.068
4.032
4.023
3.989
3.902
3.858
3.745
3.653
3.633
3.607
3.559
1.939
1.486
BRUKER
g,h
OH
c
c
O
a
a
a
i
O
O
f
e
d
N
b
O
O
7.0
6.5
6.0
5.5
5.0
4.5
4.0
3.5
3.0
2.5
2.0
ppm
1.00
1.00
0.93
2.01
2.09
2.60
6.19
3.00
8.66

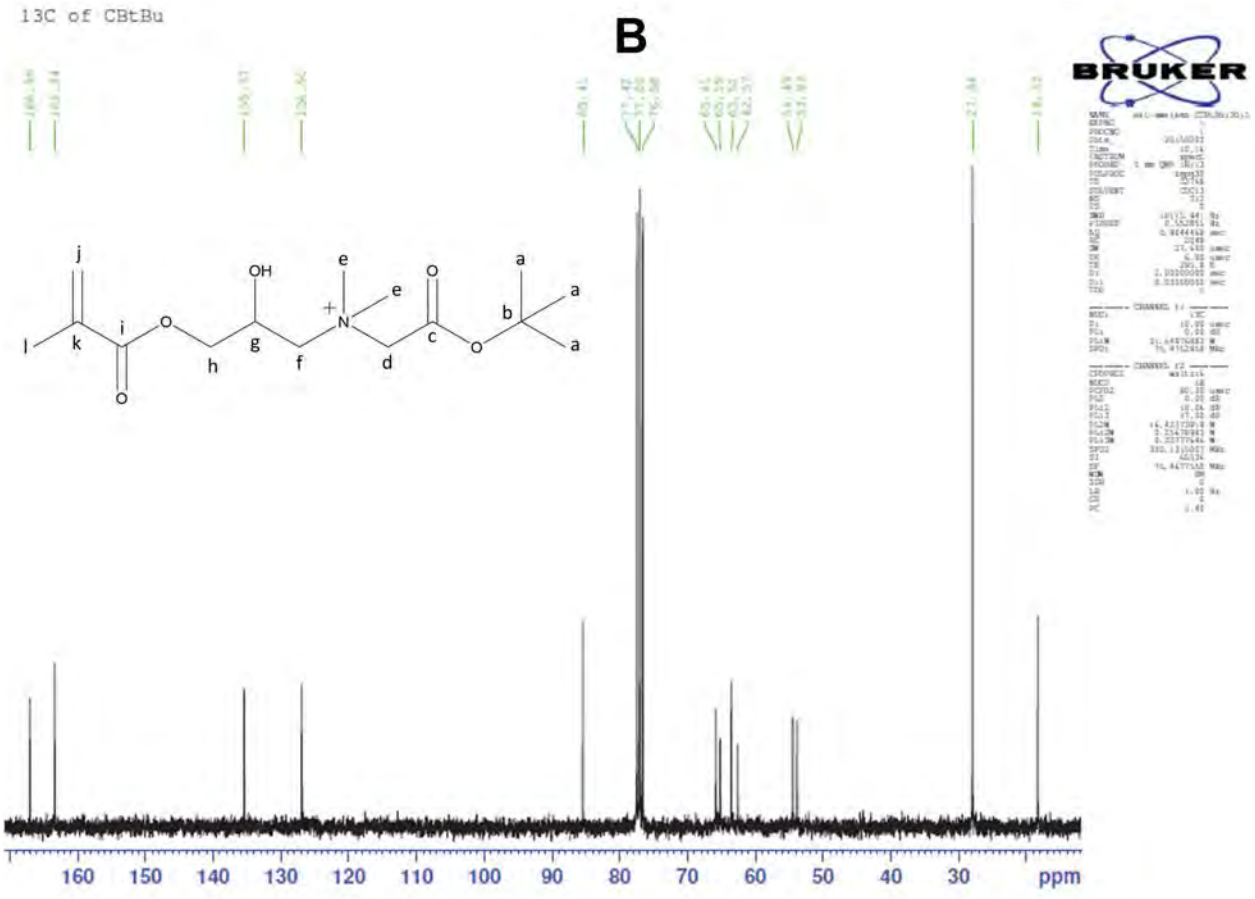

Figure S4. (A) 1H-NMR spectrum and (B) 13C-NMR spectrum of protected monomer CBtBu. CBtBu was dissolved in chloroform-d at a concentration of 50 mg/mL. Lowercase letters were assigned to each proton and carbon type as specified in each spectrum.

CBOH Synthesis

CBtBu was dissolved and reacted with TFA (2 mL TFA/g CBtBu) for 2 h under stirring. The reaction solution was precipitated in diethyl ether. The precipitate was dissolved in 100-150 mL water and reacted with Amberlite® IRA-400 hydroxide form (1 meq resin:1.01 mmol CBtBu) for 30 min in an ice bath under stirring. The resin was filtered out (same filter paper as above) and the undesired residual organics were extracted out with DCM (1:1 v/v, 3 times). The

remaining aqueous solution was frozen and placed in a freeze-dryer (VirTis 6KBTEL-85) for 3-4 days to remove the water and precipitate CBOH. Figure S5 depicts a typical ^{1}H-NMR and ^{13}C-NMR of CBOH. Yield was approximately 80 mol% with approximately 85% purity as determined by NMR. Cao et al. [1] provided an interpretation for each NMR spectrum, however an interpretation is provided based on the results obtained from the experiments described. The following is the interpretation of the ^{1}H-NMR spectrum in Figure S5A, with lowercase letters assigned to identify each proton type as assigned in the image: 1.88-1.89 (h), 3.26-3.41 (b), 3.64-3.94 (c), 4.11-4.24 (a), 4.23-4.33 (e), 4.39-4.59 (d), 4.79 (residual water), 5.70-5.72 (g), 6.11-6.13 (f). The following is the interpretation of the ^{13}C-NMR spectrum in Figure S5B, with lowercase letters assigned to identify each carbon type as assigned in the image: 17.30 (j), 53.1-53.7 (c), 62.11 (e), 63.83 (d), 65.30 (f), 66.33 (b), 127.43 (h), 135.34 (i), 167.12 (g), 168.97 (a). The peaks for the tert-butyl protecting group are gone, indicating that the monomer was successfully deprotected.

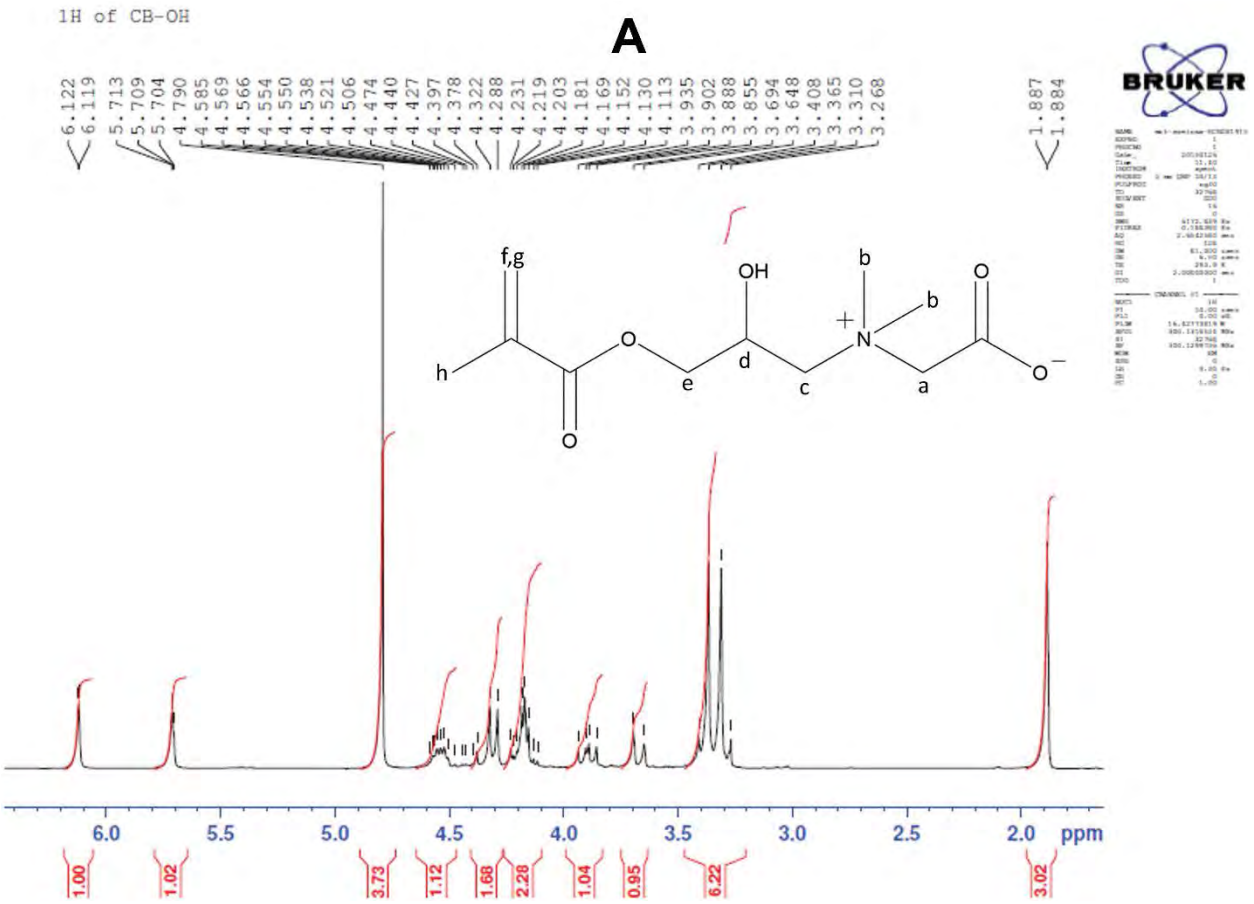
1H of CB-OH
A
BRUKER
6.122
6.119
5.713
5.709
5.704
4.790
4.585
4.569
4.566
4.554
4.550
4.538
4.521
4.506
4.474
4.440
4.427
4.397
4.378
4.322
4.288
4.231
4.219
4.203
4.181
4.169
4.152
4.130
4.113
3.935
3.902
3.888
3.855
3.694
3.648
3.408
3.365
3.310
3.268
1.887
1.884
f,g
OH
b
b
O
O
h
O
e
d
c
N
a
O
6.0
5.5
5.0
4.5
4.0
3.5
3.0
2.5
2.0
ppm
1.00
1.02
3.73
1.12
1.68
2.28
1.04
0.95
6.22
3.02

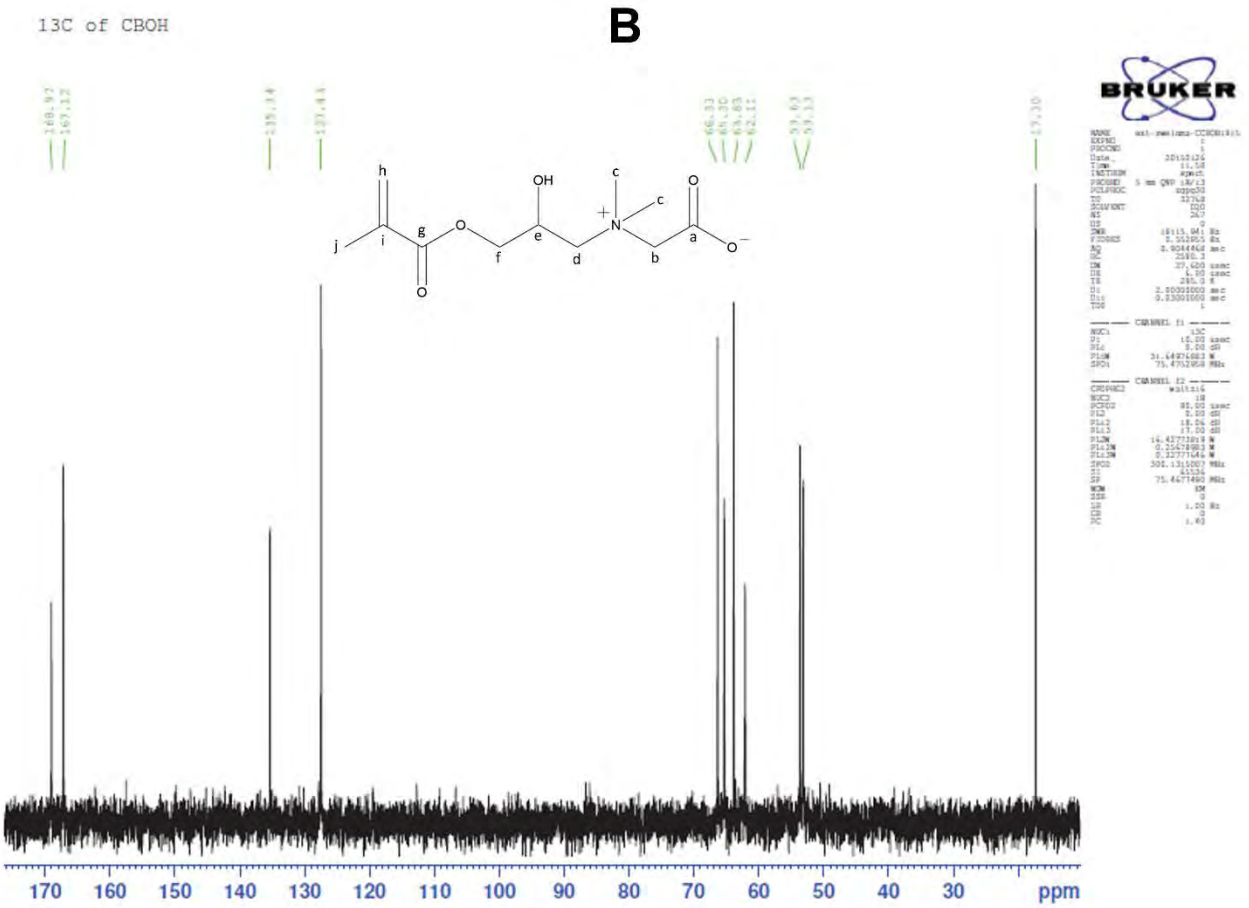

Figure S5. (A) 1H-NMR spectrum and (B) 13C-NMR spectrum of monomer CBOH. CBOH was dissolved in deuterium oxide at a concentration of 50 mg/mL. Lowercase letters were assigned to each proton and carbon type as specified in each spectrum.

CBOH Monomer Switching

NMR was used to test switching of CBOH monomer to CB-Ring. CBOH monomer was dissolved in trifluoroacetic acid-d (50 mg/mL) and ^{1}H NMR and ^{13}C NMR spectra were collected after 4 h. Figure S6 depicts the ^{1}H NMR and ^{13}C NMR spectra of CB-Ring. Cao et al. [1] provided an interpretation for each NMR spectrum, however an interpretation is provided based on the results obtained from the experiments described. The following is the interpretation of the ^{1}H-NMR spectrum in Figure S6A, with lowercase letters assigned to identify each proton

type as assigned in the image: 2.10 (h), 3.57 (sarcosine impurity of protons attached to terminal carbon(s) on the nitrogen), 3.69 (a), 4.05-4.38 (c), 4.49 (sarcosine impurity of protons attached to the carbon between the nitrogen and the carbonyl), 4.58-4.88 (b and e), 5.58-5.63 (d), 5.96 (g), 6.41 (f), 11.50 (residual trifluoroacetic acid). The following is the interpretation of the ^{13}C-NMR spectrum in Figure S6B, with lowercase letters assigned to identify each carbon type as assigned in the image: 18.79 (j), 54.46 (a), 56.68 (sarcosine impurity of terminal carbons attached to the nitrogen), 59.35 (d), 61.01 (f), 63.45 (e), 65.53 (sarcosine impurity of carbon between the nitrogen and the carbonyl), 75.50 (b), 111.4-122.7 (residual trifluoroacetic acid), 132.03 (h), 137.00 (i), 163.3-165.1 (residual trifluoroacetic acid), 165.52 (g), 170.23 (sarcosine impurity of the carbon in the carbonyl), 172.63 (c). The sarcosine impurities are seen only in this set of spectra because the switching was tested with a less pure sample as compared to the CBtBu and CBOH NMR spectra. Notice how each spectrum changed drastically from CBOH to CB-Ring, indicating a successful change in structure from CBOH to CB-Ring.

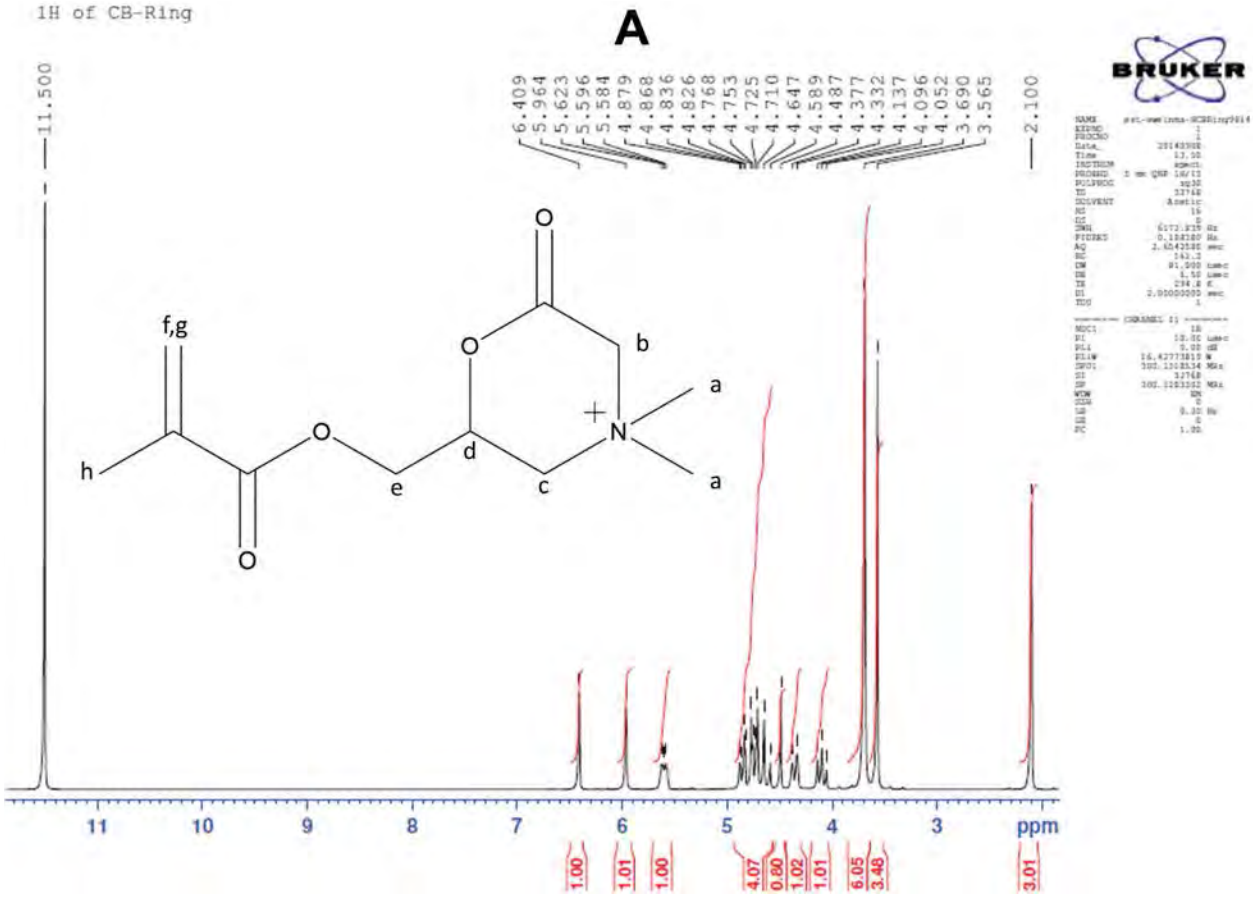
1H of CB-Ring
A
11.500
6.409
5.964
5.623
5.596
5.584
4.879
4.868
4.836
4.826
4.768
4.753
4.725
4.710
4.647
4.589
4.487
4.377
4.332
4.137
4.096
4.052
3.690
3.565
2.100
f,g
h
O
O
O
O
O
N
a
a
b
c
d
e
11
10
9
8
7
6
5
4
3
ppm
1.00
1.01
1.00
4.07
0.80
1.02
1.01
6.05
3.48
3.01
BRUKER

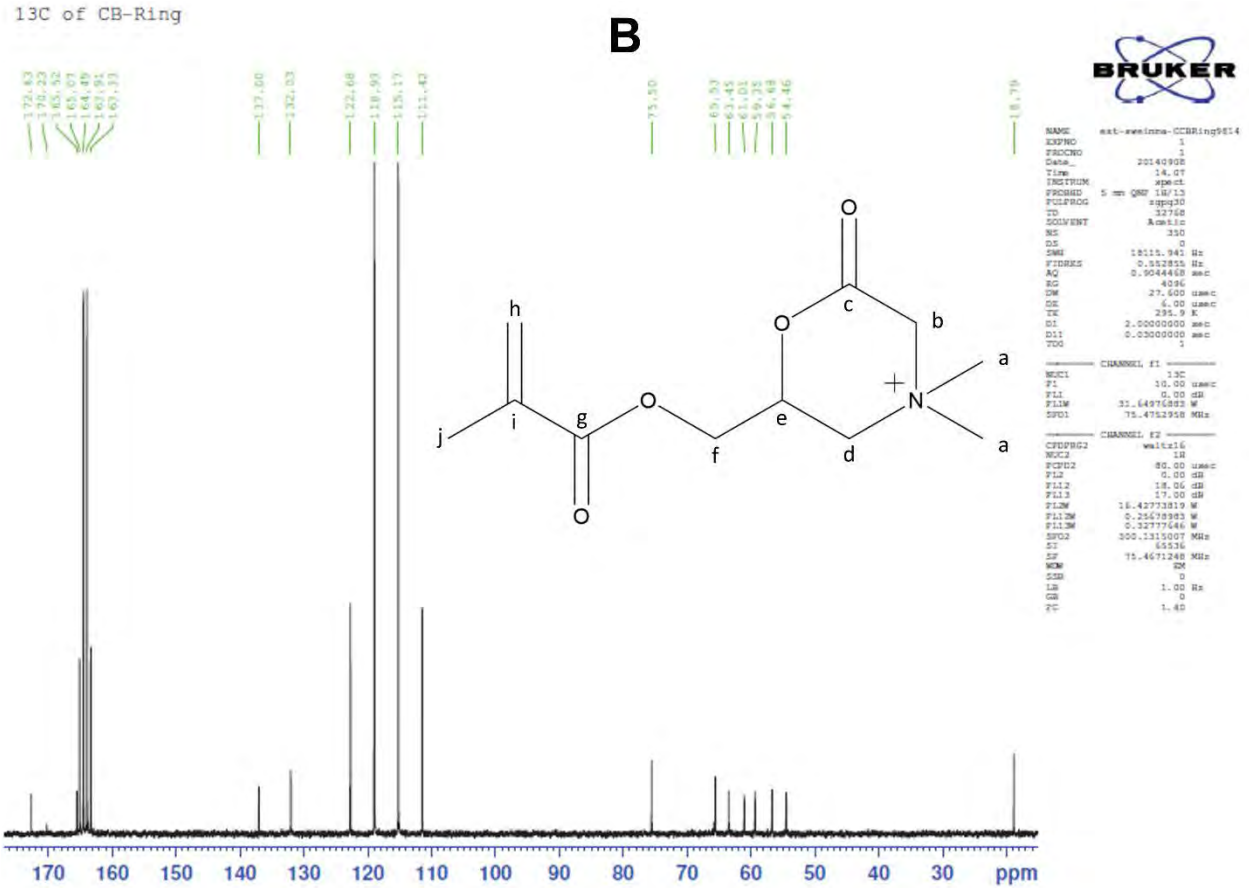

Figure S6. (A) 1H-NMR spectrum and (B) 13C-NMR spectrum of switched monomer CB-Ring. CBOH was dissolved in trifluoroacetic acid-d at a concentration of 50 mg/mL for 4 h before spectra was recorded. Lowercase letters were assigned to each proton and carbon type as specified in each spectrum.

Membrane Static Contact Angle Goniometry

Water contact angle was performed on unmodified and modified GE PES membranes and unmodified and modified Microdyn-Nadir PM UP150 PES membranes using the same procedure as described in the manuscript for the silicon wafers. GE PES membranes water contact angle was measured using a Krüss DSA100 (Freger Lab). Figure S7A shows the water contact angle

data for the GE PES membranes. The unmodified GE PES membranes had an average contact angle of 70°. The BP entrapped GE PES membranes showed a slight increase in water contact angle, while the polymer modified GE PES membranes showed a slight decrease in water contact angle. Statistically, using a t-test to compare the unmodified GE PES to the modified GE PES membranes, the BP entrapped and the poly(PEGMA) modified membranes are considered different from the unmodified membrane. Figure S7B shows the water contact angle data for the Microdyn-Nadir PES membranes. Microdyn-Nadir PM UP150 PES membranes are more hydrophilic than most common PES membranes with an average water contact angle of 51° [4-6]. Interestingly, unlike the GE PES membranes, the BP entrapped Microdyn-Nadir PES membranes had a significantly reduced water contact angle of 22°. The poly(CBOH) modified PES membranes had a water contact angle of 39°, which is similar to that of the poly(CBOH) modified silicon wafers. All three Microdyn-Nadir PES membrane data points are statistically different from each other, therefore indicating the membrane surface was further hydrophilized upon surface modification.

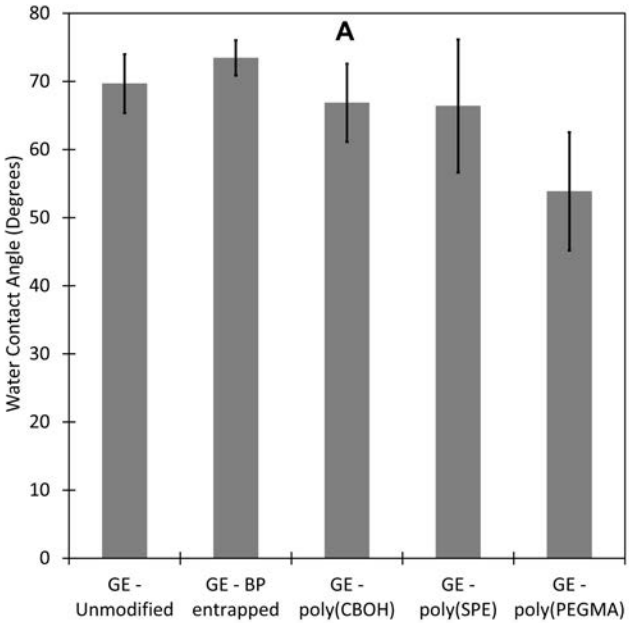

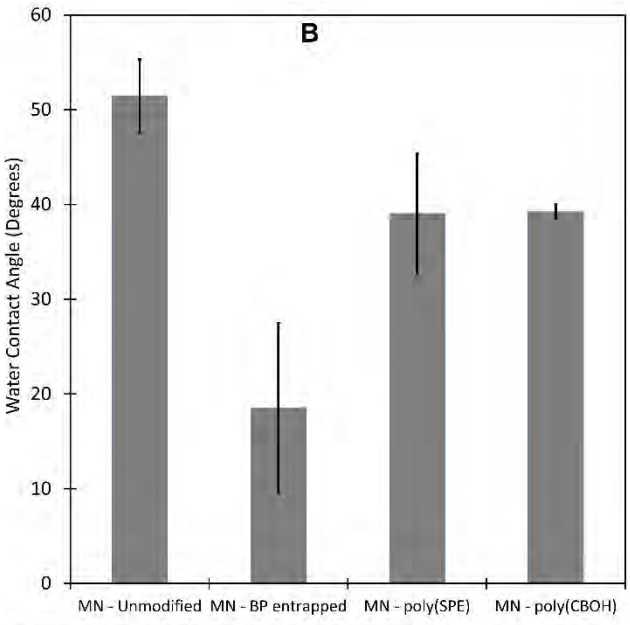

Figure S7. Water contact angle of (A) unmodified and modified GE PES membranes and (B) unmodified and modified Microdyn-Nadir PM UP150 (MN) PES membranes. Error bars represent one standard deviation among at least three samples.

Membrane Captive Bubble Contact Angle Goniometry

Air captive bubble in water contact angle measurements were performed on unmodified and modified Microdyn-Nadir PM UP150 PES membranes using a Krüss DSA 10-Mk2 contact angle goniometer. Membranes pieces were attached to a glass slide using double-sided tape and placed upside down in a clear, square petri-dish filled with deionized water, using glued glass slide pieces to suspend membrane on glass slide in the water. An air bubble was blown using a syringe underneath the membrane to allow the air bubble to interact with membrane surface. A photo was taken of each air bubble interacting with the membrane surface and the angle was measured using ImageJ software (version 1.51j8). Figure S8 shows the air-in-water captive bubble data for Microdyn-Nadir PES membranes. The data shows virtually no change in the air-

in-water captive bubble contact angle from 28° for the unmodified membrane. However, statistically using a multiple mean hypothesis test, the poly(CBOH) modified MN PES is statistically different from the unmodified MN PES.

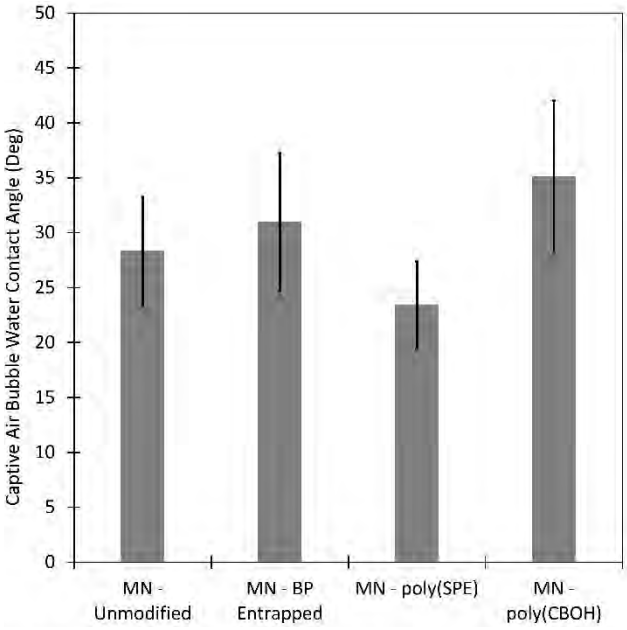

Figure S8. Captive bubble water contact angle of unmodified and modified Microdyn-Nadir PM UP150 (MN) PES membranes. Error bars represent one standard deviation among at least three samples.

Statistical Analysis

Hypothesis testing (multiple mean or t-test) was done to determine statistical relevance of the data sets. SAS® Studio (v. 3.5 enterprise edition) was used online at http://support.sas.com/software/products/ondemand-academics/#s1=2 for all statistical analyses. The Brown and Forsythe's test for homogeneity was done to test for equal variance in the multiple mean hypothesis tests. Equal variance is required to perform the multiple mean hypothesis test. All tests were done using 95% confidence ($\alpha = 0.05$); therefore, if the p-value is

greater than α then the variances or means are considered to be equal and if the p-value is less than α then the variances or means are considered to be unequal.

Water permeability statistical analysis was done using a multiple mean hypothesis test for the data in Figure 3. GE PES membranes (Figure 3A) variances were considered equal with a p-value of 0.6338. The p-value for the multiple mean test was < 0.0001, concluding at least one set of data was significantly different from the rest. Using a Tukey's t-test on the data, it was concluded that the unmodified GE PES was statistically different from the modified GE PES. The BP entrapped PES was statistically different from poly(SPE) modified PES and poly(PEGMA) modified PES. The poly(CBOH) modified PES was statistically different from poly(PEGMA) modified PES. To perform the multiple mean hypothesis test on the Microdyn-Nadir PES membranes (Figure 3B), it was necessary to take the square root of all data to obtain equal variances (p-value = 0.0079 before taking the square root and p-value = 0.0875 after). The p-value was 0.001 for the multiple mean test, concluding at least one set of data was significantly different from the rest. Using a Tukey's t-test on the data, it was concluded that the poly(SPE) modified Microdyn-Nadir PES was statistically different from the unmodified Microdyn-Nadir PES, BP entrapped Microdyn-Nadir PES, and the poly(CBOH) modified Microdyn-Nadir PES.

Bacteria deposition statistical analysis was done using a multiple mean hypothesis test for the data in Table 1. The variances were considered equal with a p-value of 0.149. The p-value for the multiple mean test was < 0.0001, concluding at least one set of data was significantly different from the rest. Using a Tukey's t-test on the data, it was concluded that unmodified PES was statistically different from the surface modified PES membranes. All the surface modified PES membranes were considered statistically the same at 95% confidence.

The biofilm volumetric quantification (no acid rinse) statistical analysis was done using a multiple mean hypothesis test for the data in Table 3. Table S1 presents the results of the statistical analysis for all nine variables. Using a Tukey's t-test on the data, it was concluded that all biovolumes, all biomass thicknesses, and no biomass roughness between the unmodified membrane and the poly(CBOH) modified or poly(SPE) modified membranes. were considered statistically different.

The biofilm volumetric quantification for poly(CBOH) modified membranes with and without acid rinse were done on the data from Table 3 and Table 4 using a pooled (equal variance) or Satterthwaite (unequal variance) two-tailed t-test. Table S2 presents the results of the statistical analysis for all nine variables. If the equal variance p-value was less than 0.05, then the Satterthwaite t-test was used, otherwise the pooled t-test was used. Dead biovolume, dead biomass thickness, live biomass thickness, and dead biomass roughness coefficient are all considered to be statistically different. Live biovolume, EPS biovolume, EPS biomass thickness, live biomass roughness coefficient, and EPS biomass coefficient are all considered to be statistically the same.

The biofilm volumetric quantification for poly(SPE) modified membranes with and without acid rinse were done on the data from Table 3 and Table 4 using a pooled (equal variance) or Satterthwaite (unequal variance) two-tailed t-test. Table S3 presents the results of the statistical analysis for all nine variables. If the equal variance p-value was less than 0.05, then the Satterthwaite t-test was used, otherwise the pooled t-test was used. EPS biovolume, dead biomass thickness, and EPS biomass thickness are all considered to be statistically different. Dead biovolume, live biovolume, live biomass thickness, dead biomass roughness coefficient,

live biomass roughness coefficient, and EPS biomass coefficient are all considered to be statistically the same.

Table S1. Statistical analysis results of the biofilm volumetric quantification between the unmodified, poly(CBOH) modified, and poly(SPE) modified Microdyn-Nadir PM UP150 PES membranes. Interpretation (what is statistically different) was done using a Tukey's t-test.

Test Variable	**Equal Variance p-value**	**Equal Means p-value**	**Statistically Different (95% Confidence)**
Dead Biovolume	0.351	< 0.0001	All
Live Biovolume	0.250	< 0.0001	Unmodified – poly(CBOH) Unmodified – poly(SPE)
EPS Biovolume	0.190	0.0012	Unmodified – poly(CBOH) poly(CBOH) – poly(SPE)
Dead Biomass Thickness	0.654	< 0.0001	Unmodified – poly(CBOH) Unmodified – poly(SPE)
Live Biomass Thickness	0.225	0.0093	Unmodified – poly(CBOH) Unmodified – poly(SPE)
EPS Biomass Thickness	0.390	< 0.0001	Unmodified – poly(CBOH) Unmodified – poly(SPE)
Dead Biomass Roughness	0.0004	N/A	N/A
Live Biomass Roughness	0.304	0.594	All Statistically the Same
EPS Biomass Roughness	0.195	0.558	All Statistically the Same

Table S2. Statistical analysis results of the biofilm volumetric quantification between the poly(CBOH) modified Microdyn-Nadir PM UP150 PES membranes with and without acid rinse.

Test Variable	**Equal Variance p-value**	**t-test used**	**Equal Means p-value**	**Interpretation (95% Confidence)**
Dead Biovolume	0.0792	pooled	< 0.0001	Statistically Different
Live Biovolume	0.0036	Satterthwaite	0.075	Statistically the Same
EPS Biovolume	0.185	pooled	0.693	Statistically the Same
Dead Biomass Thickness	0.573	pooled	0.0003	Statistically Different
Live Biomass Thickness	0.044	Satterthwaite	0.007	Statistically Different
EPS Biomass Thickness	0.038	Satterthwaite	0.894	Statistically the Same
Dead Biomass Roughness	0.143	pooled	0.022	Statistically Different
Live Biomass Roughness	< 0.0001	Satterthwaite	0.082	Statistically the Same
EPS Biomass Roughness	0.024	Satterthwaite	0.930	Statistically the Same

Table S3. Statistical analysis results of the biofilm volumetric quantification between the poly(SPE) modified Microdyn-Nadir PM UP150 PES membranes with and without acid rinse.

Test Variable	Equal Variance p-value	t-test used	Equal Means p-value	Interpretation (95% Confidence)
Dead Biovolume	0.222	pooled	0.140	Statistically the Same
Live Biovolume	0.692	pooled	0.583	Statistically the Same
EPS Biovolume	0.092	pooled	< 0.0001	Statistically Different
Dead Biomass Thickness	0.222	pooled	0.130	Statistically Different
Live Biomass Thickness	0.718	pooled	0.775	Statistically the Same
EPS Biomass Thickness	< 0.0001	Satterthwaite	0.0002	Statistically Different
Dead Biomass Roughness	0.332	pooled	0.382	Statistically the Same
Live Biomass Roughness	0.024	Satterthwaite	0.820	Statistically the Same
EPS Biomass Roughness	< 0.0001	Satterthwaite	0.113	Statistically the Same

GE PES water contact angle statistical analysis was done using a pooled (equal variance) or Satterthwaite (unequal variance) two-tailed t-test between the data for the unmodified PES and modified PES in Figure S7A. Table S4 presents the results of the statistical analysis for all tests. If the equal variance p-value was less than 0.05, then the Satterthwaite t-test was used, otherwise the pooled t-test was used. A multiple mean hypothesis test could not be done because the variances were not considered equal. Unmodified compared with BP entrapped and poly(PEGMA) are considered statistically different, while unmodified compared with

poly(CBOH) and poly(SPE) are considered statistically the same. Microdyn-Nadir PM UP150 water contact angle statistical analysis was done using a pooled (equal variance) or Satterthwaite (unequal variance) two-tailed t-test between the data for the unmodified PES and modified PES in Figure S7B. Table S5 presents the results of the statistical analysis for all tests. If the equal variance p-value was less than 0.05, then the Satterthwaite t-test was used, otherwise the pooled t-test was used. A multiple mean hypothesis test could not be done because the variances were not considered equal. All modified Microdyn-Nadir membranes were considered statistically different from the unmodified Microdyn-Nadir membranes.

Microdyn-Nadir PM UP150 air-in-water captive bubble contact angle statistical analysis was done using a multiple mean hypothesis test for the data from Figure S8. The variances were considered equal with a p-value of 0.1262. The p-value for the multiple mean test was 0.0012, concluding at least one set of data was significantly different from the rest. Using a Tukey's t-test on the data, it was concluded that unmodified PES was statistically different from the poly(CBOH) modified PES membranes at 95% confidence.

Table S4. Statistical analysis results between the water contact angle data for the unmodified and polymer modified GE PES membranes.

Test Variable	**Equal Variance p-value**	**t-test used**	**Equal Means p-value**	**Interpretation (95% Confidence)**
BP entrapped	0.103	pooled	0.019	Statistically Different
poly(CBOH)	0.705	pooled	0.349	Statistically the Same
poly(SPE)	0.186	pooled	0.488	Statistically the Same
poly(PEGMA)	0.216	pooled	0.002	Statistically Different

Table S5. Statistical analysis results between the water contact angle data for the unmodified and polymer modified Microdyn-Nadir PM UP150 PES membranes.

Test Variable	Equal Variance p-value	t-test used	Equal Means p-value	Interpretation (95% Confidence)
BP entrapped	0.0003	Satterthwaite	< 0.0001	Statistically Different
poly(CBOH)	0.1395	Pooled	< 0.0001	Statistically Different
poly(SPE)	0.0029	Satterthwaite	< 0.0001	Statistically Different

References

[1] Z. Cao, N. Brault, H. Xue, A. Keefe, S. Jiang, Manipulating Sticky and Non-Sticky Properties in a Single Material, Angewandte Chemie International Edition, 50 (2011) 6102-6104.
[2] A. Rudawska, E. Jacniacka, Analysis for determining surface free energy uncertainty by the Owen–Wendt method, International Journal of Adhesion and Adhesives, 29 (2009) 451-457.
[3] M. Kobayashi, Y. Terayama, H. Yamaguchi, M. Terada, D. Murakami, K. Ishihara, A. Takahara, Wettability and antifouling behavior on the surfaces of superhydrophilic polymer brushes, Langmuir, 28 (2012) 7212-7222.
[4] J. Haberkamp, M. Ernst, G. Makdissy, P.M. Huck, M. Jekel, Protein fouling of ultrafiltration membranes-investigation of several factors relevant for tertiary wastewater treatment, Journal of Environmental Engineering and Science, 7 (2008) 651-660.
[5] P. Kaner, D.J. Johnson, E. Seker, N. Hilal, S.A. Altinkaya, Layer-by-layer surface modification of polyethersulfone membranes using polyelectrolytes and AgCl/TiO 2 xerogels, Journal of Membrane Science, 493 (2015) 807-819.
[6] L. De Bartolo, S. Morelli, M. Rende, A. Gordano, E. Drioli, New modified polyetheretherketone membrane for liver cell culture in biohybrid systems: adhesion and specific functions of isolated hepatocytes, Biomaterials, 25 (2004) 3621-3629.